

## 20. DEEP-WATER CIRCULATION, CHEMISTRY, AND TERRIGENOUS SEDIMENT SUPPLY IN THE EQUATORIAL ATLANTIC DURING THE PLIOCENE, 3.3–2.6 MA AND 5–4.5 MA<sup>1</sup>

R. Tiedemann<sup>2</sup> and S.O. Franz<sup>2</sup>

### ABSTRACT

At Sites 925–929, an orbitally tuned time scale was generated for the Pliocene from 5 to 2.5 Ma by correlating precessional magnetic susceptibility cycles to the 65°N summer insolation record that was based on the astronomical solution of Laskar et al. (1993).

Two Pliocene time intervals were investigated. The time interval from 3.3 to 2.6 Ma includes the intensification of northern hemisphere glaciation. The second interval from 5 to 4.5 Ma monitors the warmer Pliocene and is believed to reflect a major event in the closure history of the Panama Isthmus. A bathymetric comparison between sand content and carbonate accumulation records suggests that the early Pliocene was marked by stronger carbonate dissolution and a shallower lysocline than the middle Pliocene. A drastic increase in carbonate preservation occurred at about 4.6 Ma that was probably associated with the emergence of the Panama Isthmus. Variations in the lysocline depth were dominated by the 41-k.y. tilt cycle, indicating a strong coupling to high-latitude climate forcing. In contrast, the dominance of precession cycles in less undersaturated water masses well above the lysocline may indicate changes in carbonate production and carbonate flux. Middle Pliocene maxima in carbonate dissolution at 4356 m water depth lag minima of ice volume by 12 k.y. at the obliquity band, which is typical for Pleistocene Pacific records. This phase lag decreased toward shallower water depths returning to the “Atlantic type” of carbonate preservation.

Cyclic fluctuations in the supply of Amazon sediments responded with nearly equal concentration of variance to the precession and obliquity periods. The 41-k.y. fluctuations in the supply of Amazon siliciclastics may result from sea-level changes as inferred from an in-phase relationship with benthic  $\delta^{18}\text{O}$ . Benthic oxygen isotopes show no response to orbital precession. This suggests that climatological changes in South America and/or changes in the intensity of the North Brazilian Coastal Current are strong candidates in controlling the precessional flux of terrigenous material to Ceara Rise.

### INTRODUCTION

Ocean Drilling Program Sites 925–929 recovered a bathymetric transect from 3041 to 4356 m water depth in the western equatorial Atlantic and offer an excellent opportunity to reconstruct the history of deep-water circulation and chemistry as well as variations in the terrigenous sediment supply from the Amazon. Two Pliocene time intervals are investigated, that (1) monitor the major phase of Pliocene Northern Hemisphere ice growth from 3.3 to 2.6 Ma and (2) the warmer Pliocene from 5 to 4.5 Ma, which was possibly influenced by the closure of the Panama Isthmus. Carbonate, sand fraction, and stable isotope records of all sites are compared at both time intervals. High-resolution magnetic susceptibility records of these sequences show distinct cycles, which enabled correlations from site-to-site and calibrations to the orbital time scale.

#### Mechanisms of Carbonate Preservation in the Equatorial Atlantic

Temporal and spatial variations of carbonate preservation are closely linked to biogeochemical cycles that control atmospheric  $\text{CO}_2$  (Broecker and Peng, 1989). One of the primary processes that may have lowered the atmospheric  $\text{CO}_2$  during glacials has been explained by the shift in nutrients and metabolic  $\text{CO}_2$  from intermediate water depth into deep-waters (Boyle, 1988; Boyle, 1992), which, in turn, are linked to changes in biological productivity and deep circulation

(Berger, 1970; Broecker, 1982; Berger et al., 1987; Oppo and Fairbanks, 1987). Increased  $\text{CO}_2$  concentration at depth decreases carbonate ion concentration  $[\text{CO}_3^{2-}]$  and enhances carbonate dissolution in the deep ocean. As a result, the alkalinity of the ocean increases until the deep ocean  $[\text{CO}_3^{2-}]$  concentration is restored several thousand years later to its steady-state value. The glacial increase in alkalinity will draw  $\text{CO}_2$  out of the atmosphere into the ocean (Berger, 1982).

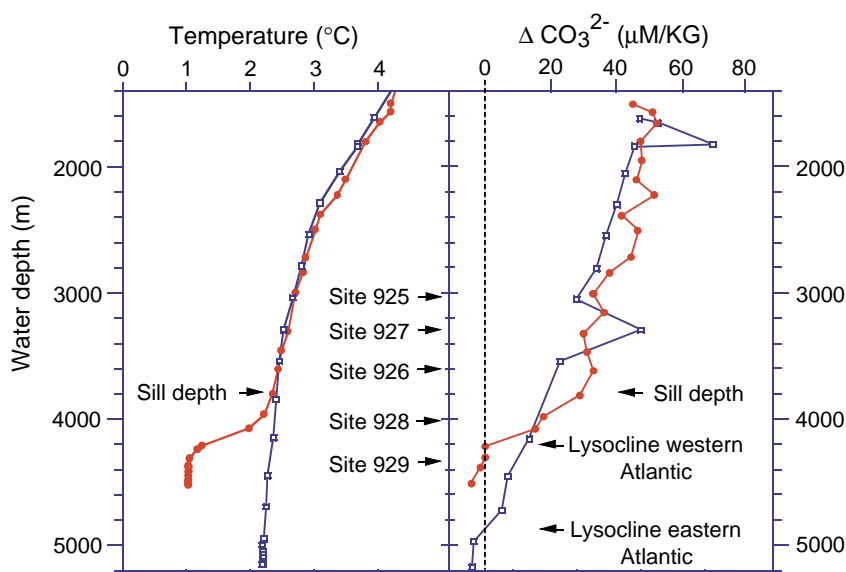
The comparison of Atlantic and Pacific carbonate dissolution records indicates, however, that dissolution changes in the two basins are out of phase during the late Neogene (Farrell and Prell, 1991), excepting the northwest Pacific (Haug et al., 1995). In contrast to the Atlantic, glacial carbonate preservation was higher in the Pacific, which supports the hypothesis that oceanic alkalinity was higher in the glacial ocean than today (Boyle, 1988).

Today, deep-water circulation and chemistry in the western equatorial Atlantic is characterized by the co-occurrence of northern and southern source deep-waters, with North Atlantic Deep Water (NADW) overlying Antarctic Bottom Water (AABW) at depths shallower than 4000 m. At Ceara Rise, the depth of the lysocline is linked to the present mixing zone between both water masses (Fig. 1), because of the high  $[\text{CO}_3^{2-}]$  ion content of NADW and the low ion concentration of AABW (Broecker and Takahashi, 1978). It is the mixing between these water masses that controls the initial chemical properties of deep water that enters the Indian and Pacific Oceans and the eastern basins of the Atlantic. The lower  $[\text{CO}_3^{2-}]$  ion concentrations in the deep Pacific and Indian Oceans cause a shallowing of the lysocline ( $\approx 3500$  m). The deeper lysocline in the eastern equatorial Atlantic basins results from the barrier of the Mid-Atlantic Ridge (MAR), which restricts the entrance of AABW from the western into the eastern basins below a sill depth of approximately 3750 m. Thus, vertical migrations of the mixing zone between northern and southern source deep-water, which can be monitored at Ceara Rise, are espe-

<sup>1</sup>Shackleton, N.J., Curry, W.B., Richter, C., and Bralower, T.J. (Eds.), 1997. *Proc. ODP, Sci. Results*, 154: College Station, TX (Ocean Drilling Program).

<sup>2</sup>GEOMAR Forschungszentrum für marine Geowissenschaften, Wischhofstraße 1-3, D-24148 Kiel, Federal Republic of Germany. rtiedemann@geomar.de

Figure 1. Depth distribution of Sites 925–929 and comparison of temperature ( $^{\circ}\text{C}$ ) and  $\Delta\text{CO}_3^{2-}$  profiles (Broecker and Takahashi, 1978) between the western (open symbols) and eastern (solid symbols) equatorial Atlantic. ( $\Delta\text{CO}_3^{2-}$  is the difference between the in situ  $[\Delta\text{CO}_3^{2-}]$  of seawater and the saturation  $[\Delta\text{CO}_3^{2-}]$  for calcite at the same temperature and pressure conditions). Today the deep-water below 4000 m is warmer and less corrosive to carbonate in the eastern Atlantic than water at comparable depth in the western Atlantic, because the flow of Antarctic bottom water (below 4000 m) from the western basin into the eastern basin is restricted by the topographic barrier of the Mid-Atlantic Ridge with a sill depth of approximately 3750 m (Metcalfe et al., 1964).



cially crucial for changes in the deep-water chemistry in the eastern equatorial Atlantic.

Several studies have demonstrated, for the late Quaternary, how deep-water circulation and chemistry in the equatorial Atlantic changed during glacial maxima (e.g., Oppo and Fairbanks, 1987; Curry and Lohmann, 1990; Bickert, 1992; Sarnthein et al., 1994; Beveridge et al., 1995). In response to a decreased production of glacial NADW, a shoaling of the mixing zone (lysocline) above the sill depth of the MAR caused increased carbonate dissolution and a strong geochemical similarity between the eastern and western Atlantic basins.

Early Pliocene changes in the deep-water circulation and chemistry in the equatorial Atlantic are not well known yet. Most Pliocene proxy records cover the major phase of northern hemisphere ice growth from 3.2 to 2.5 Ma and indicate an increased influence of carbonate-aggressive, southern-source deep-water in the equatorial Atlantic along with the intensification of Northern Hemisphere glaciation (Curry and Miller, 1989; Raymo et al., 1992). This mid-Pliocene decrease in carbonate preservation is observed in the South (Turnau and Ledbetter, 1989) and North Atlantic (Ruddiman et al., 1987; Raymo et al., 1989). Several studies have shown carbonate variations to be coherent with ice volume variations, with carbonate lagging ice volume by 6–15 k.y. (Moore et al., 1977; Peterson and Prell, 1985; Farrell and Prell, 1989; Le and Shackleton, 1992; Hagelberg et al., 1995). This time lag may represent the response time of  $[\text{CO}_3^{2-}]$  compensating for changes in alkalinity.

Moreover, other factors such as, the closure of the Panama Isthmus during the middle-early Pliocene or late Miocene (Keigwin, 1982; Keller et al., 1989), may have intensified the NADW production and thereby carbonate preservation, according to model results of Maier-Reimer et al. (1990). The model predicts a decrease in NADW production for an open isthmus and lower carbonate preservation in the Atlantic. Late Neogene changes in carbonate preservation may also be linked to long-term changes in oceanic input of  $\text{Ca}^{2+}$  from rivers, draining regions of rapid tectonic uplift, like the Amazon.

### Factors Controlling Amazon Sediment Discharge to Ceara Rise

Today, the Amazon drainage basin is one of the largest in the world. Variations in the supply of terrigenous material from the Amazon to the Ceara Rise may provide important information about con-

tinental climate variability. Strong fluctuations in the supply of Amazon sediments into the western Atlantic have been reported for the late Neogene (Flood, Piper, Klaus, et al., 1995). So far, however, it is not clear to what extent the variations in river input may reflect changes in continental South American climate. Compared to paleoclimate reconstructions of equatorial Northwest Africa, only little is known about the climatic record of the Amazon basin. Marine and continental pollen records and lake level records suggest, that, during glacial intervals, the vast tropical rain forest shrank, and savannah was an important type of vegetation in the Amazon basin because of lowered temperatures and precipitation (for an overview, see Van der Hammen and Absy, 1994). As a result, the Amazon basin rivers carried little water and sediment during glacials. In contrast, the Amazon sediment discharge into the Atlantic was higher during glacials (Flood, Piper, Klaus, et al., 1995). Sediment records from the deep sea fan provide evidence that fluctuations in the supply of Amazon sediments into the western Atlantic were mainly controlled by glacio-eustatic sea-level fluctuations (Flood, Piper, Klaus et al., 1995). Increased supply of terrigenous siliciclastics during glacial times may be linked to low sea-level stands when the Amazon river crossed the emerged shelf and discharged sediments directly into the open Atlantic. On the other hand, Showers and Bevis (1988) reported a planktonic  $\delta^{18}\text{O}$  freshwater spike for the last deglacial period (Termination I) that was found in a  $^{14}\text{C}$ -dated piston core from the upper fan of the Amazon Cone. This was interpreted to reflect an increased deglacial Amazon freshwater discharge to the equatorial Atlantic Ocean, which may result from increased pluvial activity rather than from tropical glacier melting (northern to central Andes) during deglaciation. This is corroborated by the results of Jones and Ruddiman (1982), suggesting that the Amazon plume, extending northwestward into the Caribbean, was the largest deglacial tropical freshwater source as a result of enhanced rainfall runoff.

Moreover, climate-induced variations in the west equatorial surface current system may play an important role in controlling the transport of Amazon sediments to Ceara Rise, because Ceara Rise is located about 800 km northeast from the Amazon Delta. Today, the Amazon River plume is advected along the coast northwestward with the North Brazilian Coastal Current (NBCC). When the Amazon discharge rate reaches its maximum (May–July), the NBCC veers offshore near  $5^{\circ}\text{N}$  (above Ceara Rise) to feed the eastward flowing North Equatorial Countercurrent (NECC) during June–December (Nittrouer and DeMaster, 1986; Philander and Pacanowski, 1986; Richardson and Walsh, 1986) (Fig. 2). This flow pattern coincides with

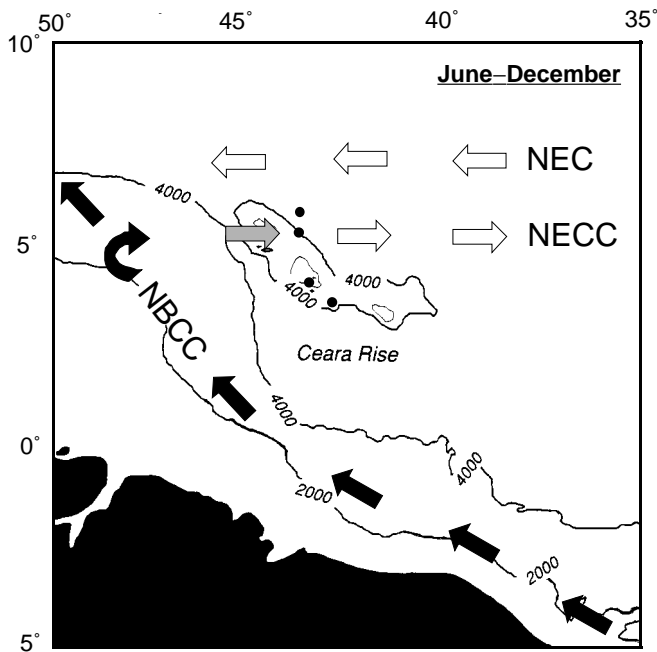


Figure 2. Schematic presentation of the modern surface circulation in the western equatorial Atlantic for the second part of the year, when the ITCZ reaches its northernmost position and the NBCC retroflects into the eastward-flowing NECC. During the first part of the year, the NBCC continuously flows northward along the coast into the Gulf of Mexico and the westward flowing NEC dominates the Ceara Rise region. (ITCZ = intertropical convergence zone, NBCC = North Brazilian Coastal Current, NECC = North Equatorial Countercurrent, NEC = North Equatorial Current.)

a sea-surface salinity minimum (anomaly) extending to Ceara Rise at the end of the summer (Dessier and Donguy, 1994). During the first half of the year, when the intertropical convergence zone (ITCZ) has its southernmost position, the NECC does not exist and the NBCC flows continuously along the coast into the Gulf of Mexico. Hence, the amount of the advection of Amazon discharge at Ceara Rise depends on the paleofluctuations of Amazon outflow as well as the latitudinal paleoposition of the ITCZ, which controls the initiation of the NECC.

## METHODS AND DATABASE

The high-resolution magnetic susceptibility and reflectance records (Curry, Shackleton, Richter, et al., 1995) were used for between-hole correlations to reconstruct a continuous composite record for each site. In general, we used the composite depth sections reported by the Leg 154 shipboard party (Curry, Shackleton, Richter, et al., 1995). However, careful inspection of the fluctuations in our carbonate records suggested a revision of composite depth intervals at Sites 925, 928, and 929 (Fig. 3A–C). The revised interpretation of the between-hole correlation patterns deleted previous discrepancies that occurred by correlating marked short-term fluctuations in the magnetic susceptibility and carbonate records between sites.

The  $\delta^{18}\text{O}$  and  $\delta^{13}\text{C}$  values of the benthic foraminifers were measured according to the standard techniques at the University of Bremen. The samples were freeze-dried, weighed, and wet-sieved through a 63- $\mu\text{m}$ -mesh sieve. The sand fraction was dried, weighed, and then dry-sieved at intervals of 150, 250, 315, and 500  $\mu\text{m}$ . The content of the sand fraction >63  $\mu\text{m}$  is given as percent of total  $\text{CaCO}_3$  because the sand fraction consists of nearly 100% carbonate

and to compensate for dilution effects caused by noncarbonate diluents. Benthic foraminifers were picked from the 250- to 500- $\mu\text{m}$  size fraction. For isotope analysis, the epibenthic species *Cibicidoides wuellerstorfi* and *Cibicidoides kullenbergi* were preferred because various studies demonstrated that the  $\delta^{13}\text{C}$  values of these species are approximately equal to bottom water  $\delta^{13}\text{C}$  (dissolved inorganic carbon) and, thus, are a good proxy for reconstructions in deep-water ventilation (e.g., Farrell, 1991; McCorkle and Keigwin, 1994). The  $\delta^{18}\text{O}$  values were adjusted to seawater equilibrium by adding 0.64 ‰ (Shackleton and Hall, 1984). At intervals where the above species were absent in the sediments, *Uvigerina* spp., *Oridorsalis umbonatus*, and *Pyrgo murrhina* were analyzed to obtain complete isotope records ( $\delta^{13}\text{C}$  records are based solely on values from *C. wuellerstorfi*). Parallel measurements to *C. wuellerstorfi* were carried out to correct the  $\delta^{18}\text{O}$  values for interspecific isotope differences. We found no significant  $\delta^{18}\text{O}$  difference between *Uvigerina* spp., *O. umbonatus*, and *P. murrhina*. If possible, 3–6 specimens were selected for each isotope analysis; some single measurements were made on *C. wuellerstorfi*.

The  $\text{CaCO}_3$  contents were determined by infrared absorption of total  $\text{CO}_2$  (organic and inorganic carbon) released by combustion with a LECO-Analyzer. At Sites 926 and 927, organic carbon contents are lower than 0.3% during the Pliocene time intervals. Hence, carbonate percentages may be overestimated by maximally 2.5% (equal to 0.3%  $C_{\text{org}}$ ). The organic carbon content was measured directly on the carbonate-free residue of the samples.

The siliciclastic fraction (100% – % $\text{CaCO}_3$ ; biogenic opal and volcanic glass are negligible) at Ceara Rise is considered to reflect the terrigenous sediment supply from the Amazon. Actually, the contribution of terrigenous material from the Amazon may be slightly overestimated when considering a few percent of aeolian sediment supply from northwest Africa to Ceara Rise. Today, about 10% of the Saharan dust that crosses the west coast of Africa is transported across the tropical Atlantic to South America during boreal winter, when the intertropical convergence zone reaches its southernmost position (Carlson and Prospero, 1972).

Mass accumulation rates ( $\text{g/m}^2/\text{yr}$ ) were calculated as the product of sedimentation rates ( $\text{cm/k.y.}$ ), percentages of the individual compounds, and dry bulk density values. Dry bulk density values were calculated from the GRAPE (Gamma-Ray Attenuation Porosity Evaluator) density data, using the following equation (Curry, Shackleton, Richter, et al., 1995):

$$\text{dry density} = \frac{\text{GRAPE density} - \text{water density}}{\text{grain density} - \text{water density}} \times \text{grain density}.$$

The pore-water density was set to 1.035  $\text{g/cm}^3$ , according to a mean salinity value of 35‰. Grain density values were measured downcore at discrete samples aboard the *JOIDES Resolution* with irregular distances of 2–3 m and were interpolated for our sample depths. The GRAPE density data were measured every 1 to 3 cm. The estimated dry bulk density data reproduced the measured in situ data to within a standard error of 0.02  $\text{g/cm}^3$ . The use of accumulation rates compensated the effect of percentage dilution by different sediment components.

For spectral analyses, we used the standard techniques of Imbrie et al. (1984). For spectral estimates as a function of depth, the proxy records were interpolated at 10-cm intervals. For spectral analyses in the time domain, the age of each data point was estimated by linear interpolation between age-depth control points. We then interpolated each record at constant 3-k.y. intervals. After the data had been linearly detrended, the spectra, coherencies, and phase angles between two signals over a given frequency band were estimated (confidence level of 80%). The number of lags of the cross-correlation function was set to 90 (70) for the time interval 3.35–2.6 Ma (4.94–4.4 Ma) having at least 7 degrees of freedom. The average sample spacing for

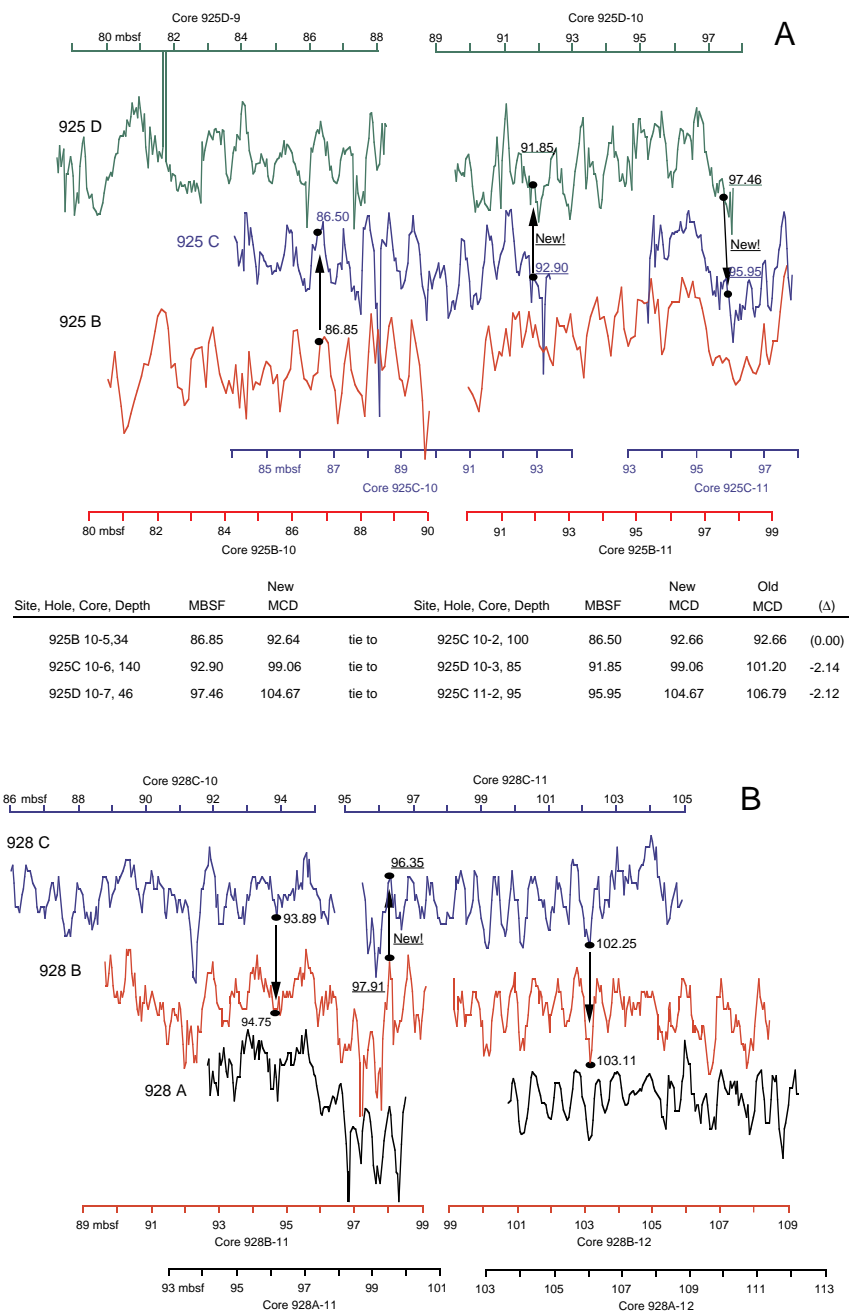


Figure 3. Revision of composite depth intervals based on reinterpretations of between-hole correlation patterns using magnetic susceptibility and reflectance records. **A.** Site 925. **B.** Site 928. **C.** Site 929. Depth scales are given in mbsf. Arrows and depth values (mbsf) indicate switch points between composite depth sections. Tables beneath figure panels summarize changes and new “pathways” for generating the composite depth.

isotope, carbonate, and sand fraction analyses is 10 cm at all sites and corresponds to a mean time resolution of 3.5 k.y. (yielding a Nyquist period of 7 k.y.). At Site 929, strong carbonate dissolution events during the early Pliocene time interval occasionally caused low sedimentation rates of about 1 cm/k.y. and decreased the sample spacing to about 10,000 yr.

### Astronomical Calibration of the Pliocene Time Scale (5–2.5 Ma)

At Ceara Rise, the opportunities for an astronomical calibration of the Pliocene time scale are excellent, as the composite sections at all sites are characterized by high-frequency, cyclic variations in lithology

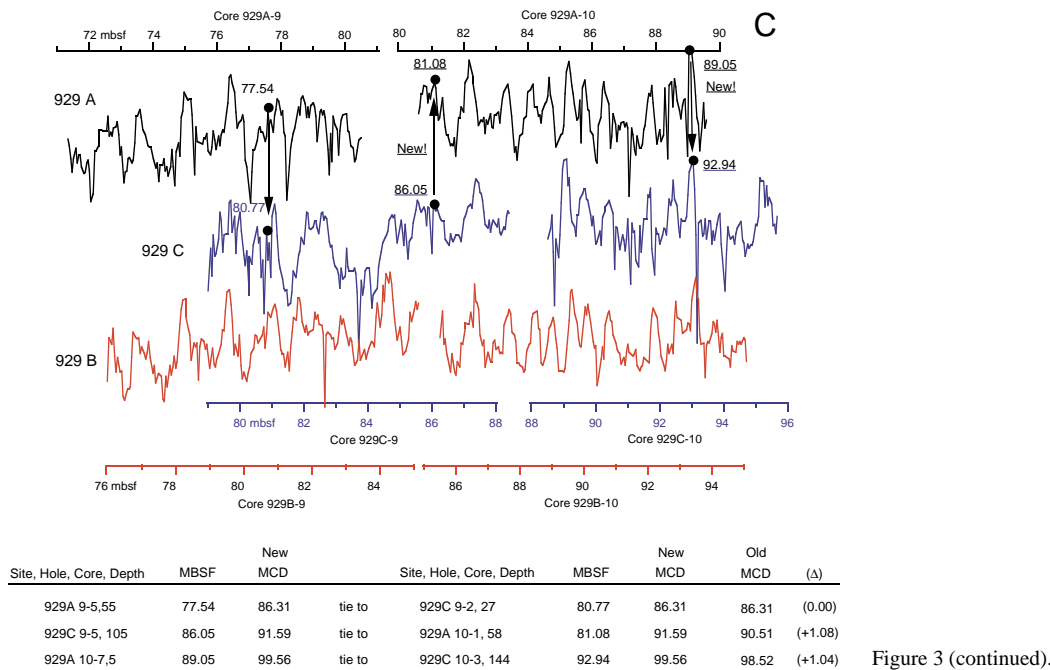


Figure 3 (continued).

caused by high-amplitude changes in the ratio of carbonate and terrigenous sediments. The existing, orbitally derived age models for the Pliocene from 5 to 2.5 Ma are almost identical (Hilgen, 1991; Shackleton et al., 1995; Tiedemann et al., 1994; Lourens, 1994) and have been calibrated to the astronomical solution of Berger and Loutre (1991), (Ber90). Recently, Lourens et al. (1996) demonstrated, however, that unrealistic large time lags will occur between obliquity and the obliquity-related variations in the proxy records, if the orbital data from Berger and Loutre (1991) are used as a tuning target. Lourens et al. pointed out that the geological record can be calibrated most accurately to the summer insolation record calculated from the Laskar (1990) solution  $La90_{(1,1)}$  with a dynamically ellipticity of the Earth of 1 and a tidal dissipation term of 1, both close to present-day values. The advantage of the  $La90_{(1,1)}$  solution is that it considers the chaotic motion of the Earth (caused by perturbation effects of Jupiter and Saturn) more accurately. Hence, we prefer the astronomical solution of Laskar (1990) to that of Berger and Loutre (1991) for the tuning procedure. Differences between the astronomical solutions of Ber90 and  $La90_{(1,1)}$  are small in the middle Pliocene but increase towards the early Pliocene. The obliquity of Ber90 leads those from  $La90_{(1,1)}$  by 7 k.y. at 2.5 Ma and by 22 k.y. at 5 Ma. At precession, Ber90 leads  $La90_{(1,1)}$  by 3 k.y. at 2.5 Ma and by 10 k.y. at 5 Ma.

To be consistent with the astronomical calibration of the Pleistocene and Miocene sediment profiles from Ceara Rise (Bickert et al., Chapter 16, this volume; Shackleton and Hall, this volume), we used the same target record ( $65^{\circ}N$  summer insolation, based on orbital data from  $La90_{(1,1)}$ ). As the tuning medium, we used the high-resolution magnetic susceptibility records, which are indicative of fluctuations in the supply of terrigenous sediments (e.g., Robinson et al., 1995). The tuning concentrated on Site 926 (3598 m water depth), because high-resolution biostratigraphic studies focused on this site to calibrate the Pliocene and Miocene nannofossil and foraminiferal events to the orbitally tuned time scale at Ceara Rise. The age model for Site 926 was then transferred to the other sites by correlating the magnetic susceptibility records (Fig. 4).

The first step toward astronomical calibration was to examine the cyclic fluctuations of the magnetic susceptibility in the depth domain, because the Pliocene sedimentation rates were expected to show only little variability of 2.5–3.5 cm/k.y. as inferred from the initial biostratigraphic age model (Curry, Shackleton, Richter, et al., 1995). Hence, if the fluctuations of the magnetic susceptibility were strongly controlled by the main orbital cycles of obliquity and precession, then dominant susceptibility cycles with wave lengths of 103–144 cm (obliquity forcing) and 55–77 cm (precession forcing) are expected. Frequency spectra of magnetic susceptibility fluctuations (Fig. 5) exactly reflected these cycles with dominant wave lengths of 105–135 cm and 55–70 cm over the Pliocene depth interval, 78–154 m composite depth (mcd), which represents the time interval from 5 to 2.5 Ma. After filtering in the depth domain, we found a good match in amplitude variations between orbital precession and the precession-related filter outputs (55-cm and 70-cm cycles). These filter outputs were used to generate a time scale that brings the filtered cycles into phase with the inferred astronomical forcing. Magnetic susceptibility maxima ( $CaCO_3$  minima) were tuned to northern hemisphere insolation minima, assuming no phase difference (Fig. 6). This negative correlation was indicated by the benthic oxygen isotope records from Site 926 (3.3–2.6 Ma; 5–4.5 Ma), which clearly indicated that magnetic susceptibility maxima occurred during cold stages. The assumption of zero phase differences might be an oversimplification of the true phase relationships between the magnetic susceptibility record and the insolation record, but small phase differences for the early and middle Pliocene would only result in a minor error of the tuned time scale.

After tuning the magnetic susceptibility minima to insolation maxima, the susceptibility record from Site 926 was filtered again in the time domain at the main orbital frequencies. The amplitude variations of orbital precession and the 22-k.y.-filter output are characterized by a remarkable similarity, suggesting that we correctly mapped the climate signal onto the orbital record (Fig. 6). The 41-k.y.-filter output appeared to be in phase with orbital obliquity (Fig. 6). Cross-

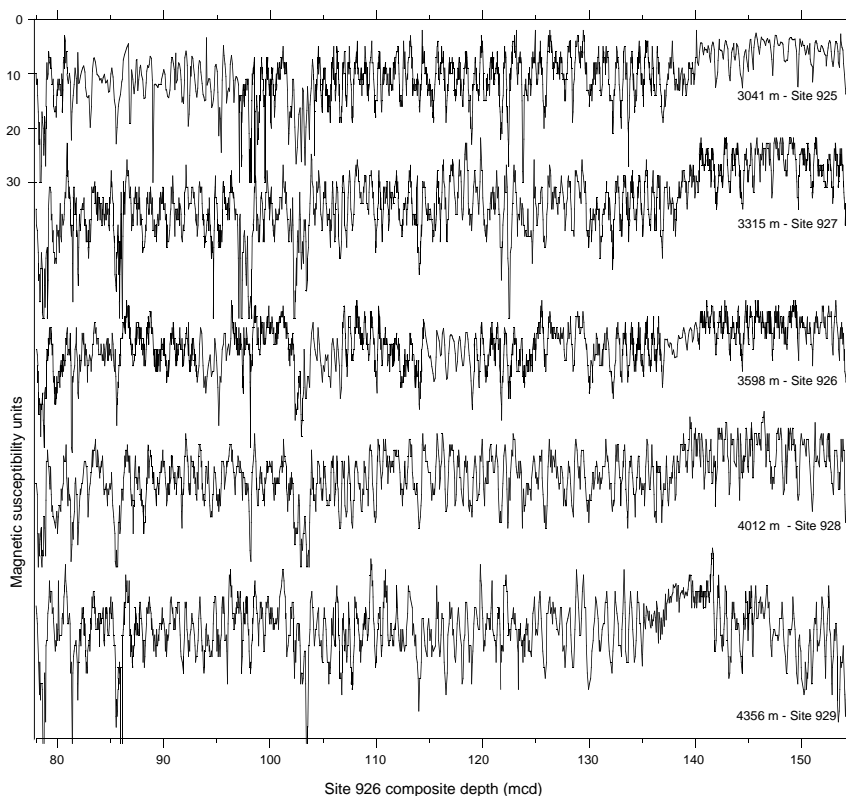


Figure 4. Correlation of magnetic susceptibility records from the Ceara Rise depth transect. Depth scales are adjusted to the Site 926 composite depth.

spectral comparison indicated that northern hemisphere insolation and magnetic susceptibility were exactly in antiphase (Fig. 7) and displayed high coherencies at the precessional (0.95 and 0.93) and obliquity (0.90) frequency bands. After transferring the age model to the other sites by correlating sequences of distinct magnetic susceptibility fluctuations (Fig. 4), the sedimentation rates were found to vary from 2 to 4 cm/1000 years at the shallower sites 925–927 (Fig. 6). The deeper Sites 928 and 929 show lower values and larger fluctuations of 1–3.6 cm/k.y., reflecting changes in carbonate preservation. At Site 929, uncertainties in the age model may occur between 4.55 and 4.3 Ma (Fig. 4; 137–143 mcd), because extremely low-amplitude fluctuations in the magnetic susceptibility record indicated no clear cyclicity or prominent structures that could be correlated to other sites. In the time interval from 5 to 4.55 Ma, the structure of the magnetic susceptibility fluctuations (as well as the variability of the reflectance record; not shown) deviated also markedly from the other sites, although a distinct cyclicity occurred. For this reason, we correlated the carbonate record from Site 929 to the other sites and transferred a few age control points of prominent carbonate minima, before tuning the rest of the interval separately.

## RESULTS

### Oxygen and Carbon Isotopes

For comparison, the benthic  $\delta^{18}\text{O}$  records from Site 926 are plotted vs. the benthic  $\delta^{18}\text{O}$  records from the subtropical northeast Atlantic (Site 659; Tiedemann et al., 1994) and the eastern equatorial Pacific (Site 846; Shackleton et al., 1995), which have independently tuned time scales (based on the Ber90 time scale). During the time interval from 3.3 to 2.6 Ma (Fig. 8A), isotope stages G2 to M2 are easily recognized at Site 926 and are well correlated with the isotope records from Sites 659 and 846. During the early Pliocene from 5 to 4.4 Ma (Fig. 8B), the prominent isotope events Si4 and Si6 occurred

at Site 926 about 20 k.y. earlier, as well as one obliquity cycle earlier, than at Sites 659 and 846. This offset results from the phase differences for obliquity and precession, if the La90<sub>(1,1)</sub> solution is applied instead of the Ber(90) solution.

Spectral analyses of the  $\delta^{18}\text{O}$  record from Site 926 indicate the Pliocene dominance of the obliquity period (Fig. 9), which have been shown to be typical for Atlantic and Pacific benthic isotope records (Shackleton et al., 1995; Tiedemann et al., 1994). At precessional periods, the variance is less than 5%. Cross-spectral analyses reveal that the oxygen isotope fluctuations tend to lag northern hemisphere summer insolation by  $1 \pm 1$  k.y. (middle Pliocene) and  $2.5 \pm 1$  k.y. (early Pliocene) at the obliquity frequency band (Fig. 10). For comparison, Imbrie et al. (1984) proposed for the late Pleistocene a time lag of 8 k.y. between ice volume ( $\delta^{18}\text{O}$ ) and obliquity forcing. However, a lower time lag for the Pliocene is expected according to the model results of Imbrie and Imbrie (1980), because this estimate depends on the size of the ice sheets and would imply a lower response time (about 4 k.y.) for smaller ice sheets in the Pliocene (Chen et al., 1995). Hence, our time scale that is based on an in-phase relationship between magnetic susceptibility and summer insolation may include an error of less than 3 k.y.

The short-term amplitude variations of  $\delta^{18}\text{O}$  fluctuations at Site 926 are very similar to those at Sites 846 and 659 during the early Pliocene (Fig. 8). During the middle Pliocene, the amplitude variations are similar to those in the equatorial northeast Atlantic but exceed those at the equatorial Pacific Site 846 by about 0.5‰. This implies larger fluctuations in deep-water temperature/salinity in the equatorial Atlantic. The long-term variations between both Atlantic records appear to be different. Cycles of about 300 k.y. dominate the  $\delta^{18}\text{O}$  curve at Site 926, whereas the long-term minima show values of about 0.5‰ lower than at Site 659. This suggests different water masses for 3000 and 3600 m water depth in the equatorial Atlantic.

At Site 926, the Pliocene carbon isotopes fluctuate between 1.4 and  $-0.3$ ‰ (Fig. 8). The extreme negative  $\delta^{13}\text{C}$  excursions ( $< -0.5$ ‰)

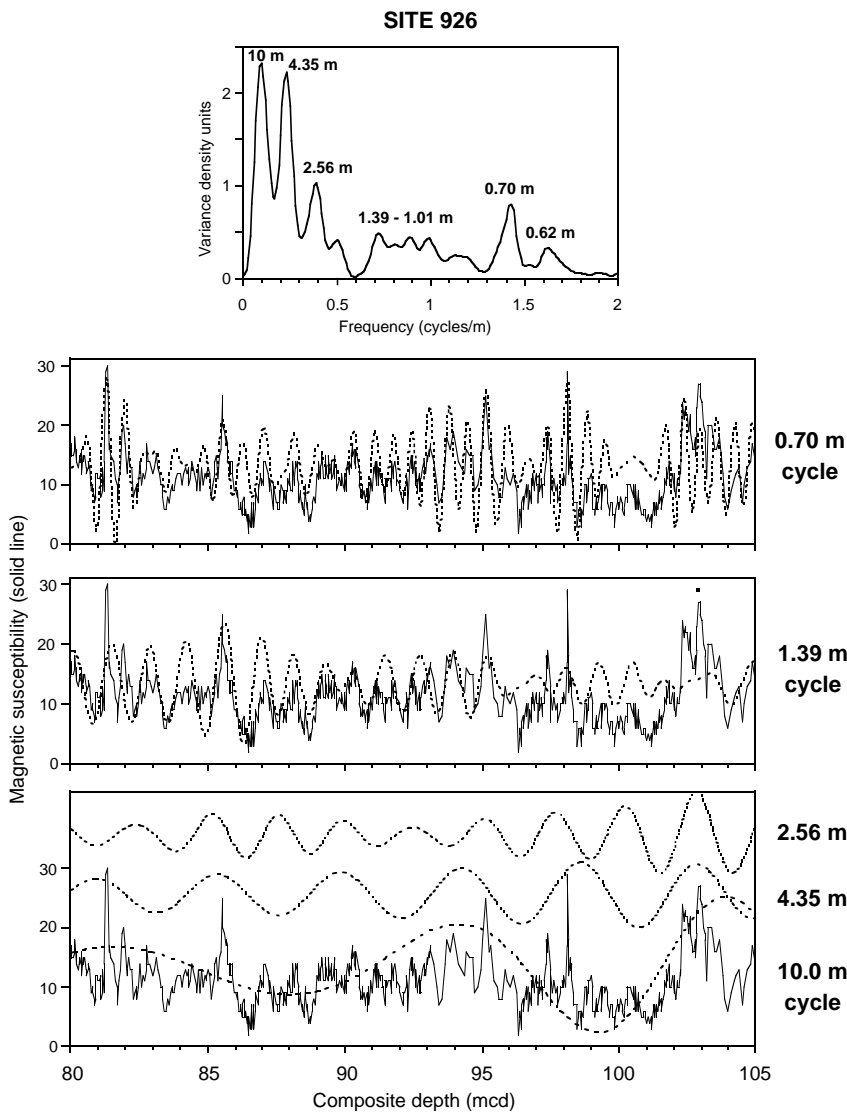


Figure 5. Frequency spectrum of magnetic susceptibility fluctuations in the depth domain, exemplified by the depth interval 139–155 mcd ( $\approx 4.5$ –5 Ma). For comparison, dominant cycles with a wavelength (in depth terms) are filtered (dashed lines) and overlain by the magnetic susceptibility record. Cycles with a wavelength of 105–135 cm and 55–70 cm are related to orbital forcing by obliquity and precession, respectively.

are regarded as less trustworthy, because they are based on single samples and are not corroborated by the next younger or older sample. Compared to the early Pliocene time interval, variations in amplitudes are higher during the middle Pliocene, when climatic differences are enhanced. The cyclic variations contain concentrated variance at the 41-k.y. obliquity band. The 41-k.y.-related  $\delta^{13}\text{C}$  maxima, indicative of deep-water ventilation maxima, lag ice-volume minima by about  $4 \pm 2$  k.y. The variance at precessional periods is lower than 5% and is not significant.

The comparison of benthic  $\delta^{13}\text{C}$  records from Ceara Rise (3598 m water depth) and the equatorial northeast Atlantic (Site 659, 3070 m water depth; Tiedemann, 1991) shows on average 0.35‰ higher  $\delta^{13}\text{C}$  values for the Ceara Rise deep-water, despite the greater water depth (Fig. 8). This may indicate that the deep-water flow in the western equatorial Atlantic is less influenced by remineralization processes. The long-term trends and the short-term variations in amplitudes, however, are similar at both sites. During the early Pliocene, both records indicate a long-term decrease in deep-water ventilation from 4.9 to 4.55 Ma, followed by an increase until 4.4 Ma. The middle Pliocene interval is marked by a gradual decrease in glacial  $\delta^{13}\text{C}$  values at Site 659 and parallels the intensification of the northern hemisphere glaciation from 3.15 to 2.5 Ma. At Ceara Rise, this trend oc-

curs later at about 2.7 Ma, when first glacial maxima occur in stages G6–G4.

### Carbonate

The bathymetric transect of carbonate records from 3000 to 4400 m water depth show broad coherency, as well as good correlation in detail, during the Pliocene time intervals (Fig. 11). In general, the deeper sites show lower values and larger fluctuations, as one would expect. Both Pliocene time intervals show an “Atlantic-type” carbonate preservation pattern with maxima during warm stages. The deep-water transect is marked by Pliocene variations in carbonate between 15% and 90%. Cyclic variations are dominated by orbital obliquity during the middle Pliocene and by precession during the early Pliocene. The most drastic change in carbonate concentrations from 30% to 60% occurs at 4.65 Ma below 4000 m water depth (Site 929); prior to 4.6 Ma, carbonate contents are lowered by factor 2.

Before reaching any conclusion, we have to consider the role of noncarbonate dilution (mainly siliciclastics). At the shallow sites, where carbonate preservation was good, changes in sedimentation rates should reflect the variability of the dominant sediment component. Low sedimentation rates during the early Pliocene are associat-

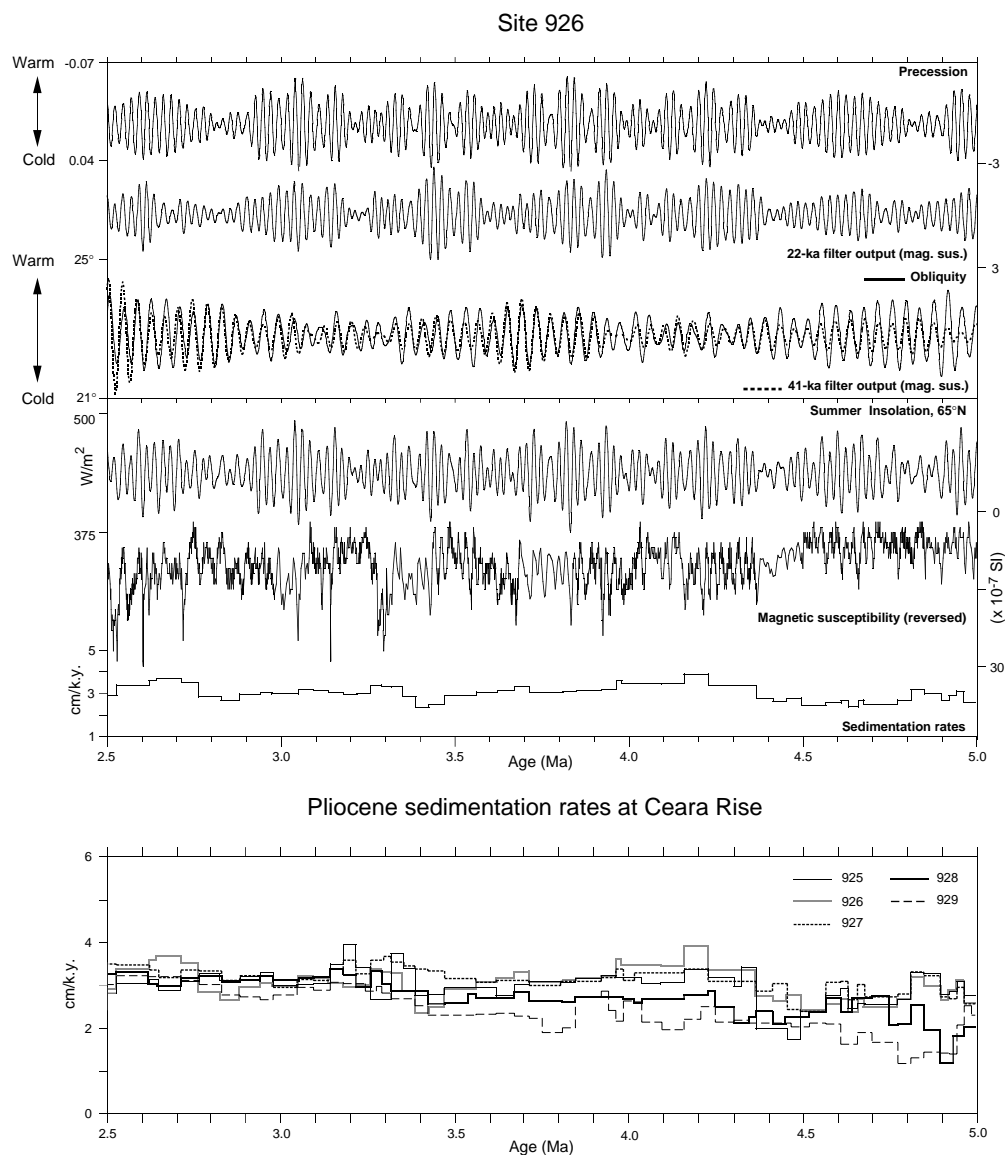


Figure 6. Site 926 time scale from 2.5 to 5 Ma based on tuning the magnetic susceptibility record to the La90<sub>(1,1)</sub> summer insolation record (65°N; Laskar, 1990). Comparison of filtered 22-k.y.- and 41-k.y.-components of magnetic susceptibility with orbital precession and obliquity. The precessional (obliquity) filter has a central frequency of 0.045 (0.0244) cycles/k.y. and bandwidth of 0.015 (0.006) cycles/k.y. Sedimentation rates are found to vary between 2 and 3.8 cm/k.y. at Site 926 and vary from 1 to 4 cm/k.y. over the entire bathymetric transect.

ed with high percentages in carbonate and high sedimentation rates during the middle Pliocene are associated with lower carbonate contents (Fig. 11A and B). This inverted pattern indicates that sedimentation rates are controlled by variations in the supply of siliciclastics. Thus, the lower carbonate contents during the middle Pliocene result from an increase in the dilution by terrigenous siliciclastics. This also explains the discrepancy in carbonate contents between Sites 926 and 927. The deeper Site 926 shows on average slightly higher carbonate concentrations. This discrepancy disappears when using carbonate accumulation rates.

The difference in carbonate accumulation between shallow and deep sites (Fig. 11) is a quantitative indicator of the amount of carbonate lost to dissolution, because all sites are located close together so that surface productivity and the carbonate flux to each site should be equal. At the shallowest Site 925 (3041 m water depth), the variability of the carbonate accumulation rates from 15 to 30 g/m<sup>2</sup>/yr

relatively uniform during the early and middle Pliocene time intervals. The deepest Site 929 (4356 m water depth), however, is characterized by distinct long-term differences in carbonate accumulation.

The Pliocene intensification of northern hemisphere glaciation from 3.15 Ma to 2.6 Ma (Fig. 8) is paralleled by decreasing carbonate accumulation rates at 4350 m water depth and an increased loss of carbonate between 3000 and 4350 m water depth (Fig. 11). The early Pliocene, from 5 to 4.57 Ma, is marked by an extremely low level of carbonate accumulation rates (7 g/m<sup>2</sup>/yr) below 4350 m water depth. At 4000 m water depth, the carbonate accumulation rates approach this level of poor carbonate preservation at 4.9 and 4.65 Ma. This early Pliocene time interval is marked by the greatest loss of carbonate (about 17 g/m<sup>2</sup>/yr) between 3000 and 4350 m water depth and a strong increase in carbonate dissolution below 3800 m. This loss to carbonate dissolution is about two times higher than during the middle Pliocene from 3.3 to 2.6 Ma. Only small differences in carbonate

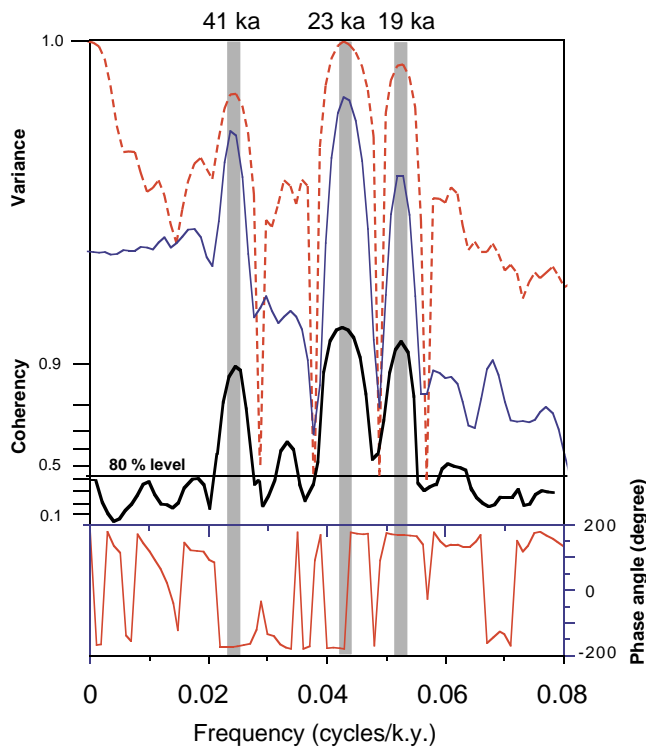


Figure 7. Top: Spectral density and cross-coherency between Northern Hemisphere summer insolation and magnetic susceptibility from Site 926 for the Pliocene from 2.5 to 5 Ma. Bottom: Phase angle vs. frequency plot (3 ka steps, 110 lags, 20 degrees of freedom).

preservation over the entire bathymetric transect occur from 4.5 to 4.4 Ma and at about 3.05 Ma.

Spectral analyses indicate that the coupling to Milankovitch forcing is strongest in the precession band during the middle Pliocene (Fig. 9). No clear response is shown for the early Pliocene.

### Sand Fraction

It has been shown that the sand content of deep-sea carbonates decreases as dissolution progresses (e.g., Yasuda et al., 1993; Bickert et al., Chapter 15, this volume), and hence, the sand content can be used as a proxy for changes in carbonate dissolution (Fig. 12). In general, the sand contents decrease with increasing water depth. The bathymetric patterns of variations in sand percentages and carbonate accumulation rates are very similar. The sand contents, however, seem to respond more sensitively to changes in deep-water carbonate saturation.

During the middle Pliocene, from 3.3 to 3.05 Ma (Fig. 12A), the sand contents are very similar between 3300 and 4000 m water depth, suggesting no significant long-term differences in carbonate preservation and a uniform water mass. From 3.05 to 2.6 Ma, the sand curve at 4000 m water depth diverges from the shallower ones, indicating a reorganization in deep-water chemistry and circulation, parallel to the intensification of northern hemisphere glaciation. This is marked by a gradual decrease in glacial sand contents and an increase in amplitude variations at 4000 m water depth, reflecting a long-term shoaling of the glacial lysocline from 3.05 to 2.6 Ma. In contrast, the level of interglacial sand values remains nearly constant and very close to that of the shallower sites, suggesting no long-term changes in carbonate preservation above 4000 m water depth during middle Pliocene warm stages. Below 4000 m, a gradual shoaling of the interglacial position of the lysocline from 3 to 2.6 Ma is indicated by a

long-term decrease in interglacial sand contents and amplitude fluctuations as monitored at the deepest Site 929 (4356 m water depth).

In contrast to the middle Pliocene, the early Pliocene from 5 to 4.4 Ma is characterized by lower sand contents and lower amplitude variations over the entire depth transect, suggesting a shallower lysocline during the early Pliocene (Fig. 12B). A dramatic highstand of the lysocline occurs at about 4.9 Ma and coincides with a pronounced  $\delta^{18}\text{O}$  cold event. From 4.95 to 4.6 Ma, the  $\delta^{18}\text{O}$  trend towards warmer climate conditions is paralleled by a slight long-term deepening of the lysocline. This is illustrated by increasing sand contents at the shallower Sites 926 and 927, and by a marked step-like increase at the deeper Site 928 at 4.6 Ma. The sand curve of the deepest Site 929 shows two steps of increased carbonate preservation, one with a first pronounced maximum at 4.6 Ma, and a second one at 4.5 Ma. Short-term fluctuations of the lysocline depth appear to be strongest at around 4000 m water depth and are characterized by high-amplitude fluctuations in the sand contents (Site 928), which correlate with the  $\delta^{18}\text{O}$  record. Peak sand content is associated with warm stages. After 4.5 Ma, the differences in the sand content decrease over the depth transect, probably indicating less stratified water masses or a higher alkalinity.

Spectral analyses indicate that the dominant variability in the sand records over the middle Pliocene interval includes Milankovitch variability at the main orbital frequencies bands of obliquity and precession (Fig. 13). The bathymetric comparison of frequency spectra between Sites 925, 927, 928, and 929 reveals a distinct shift in spectral character with increasing water depth. At the shallow Sites 925 and 927 (3041–3315 m), fluctuations in the sand content are dominated by precession cycles, whereas the deeper sand records below 4000 m water depth are dominated by obliquity cycles. The strongest response to orbital obliquity occurred at Site 928, where changes in carbonate dissolution/preservation, and thus the effects of fluctuations of the lysocline depth, are greatest. This clearly reflects the response of different aspects of the carbonate production/dissolution/preservation system at Ceara Rise. Variations in the lysocline depth and changes in deep-water alkalinity have a strong coupling to high-latitude climate forcing, whereas the dominance of the precession cycles at less-undersaturated water masses well above the lysocline may be indicative of changes in carbonate production and carbonate flux. The transition zone from precession- to obliquity-dominated frequencies is marked by no response to orbital periods during the middle Pliocene. At 3600 m water depth (Site 926), most variance of sand content variability is concentrated at periods of 56 and 37 k.y.

In addition, cross-spectral analyses were carried out between  $\delta^{18}\text{O}$  and %sand and insolation and %sand for the middle Pliocene time interval. Surprisingly, we found for the obliquity band, that carbonate preservation maxima (maximum sand content) lead ice volume minima by 7.5 ka at 4356 m water depth and that this phasing decreased towards shallower water depths (Table 1). The implications will be discussed later. Phase relationships for the precession band were estimated from cross-spectral analyses between insolation and sand contents, because the  $\delta^{18}\text{O}$  variance at precession was less than 5%. The phase relationships for the precession band indicate no water depth relationship (considering the error limits), and sand maxima slightly lag insolation maxima by about 1.5 k.y., except for the shallowest Site 925, where sand maxima lag insolation maxima by about 9.5 k.y. (Table 1).

### Organic Carbon

Organic carbon records are available from the shallow Sites 926 and 927 (Fig. 14). Both Pliocene time intervals are characterized by very low organic carbon contents of <0.3%. The fluctuations in organic carbon contents (not shown) do not indicate significant variance at 41-k.y. tilt and 23-k.y. precession cycles (Fig. 9); instead, they contain significant variance near periods of 56 and 37 k.y.,

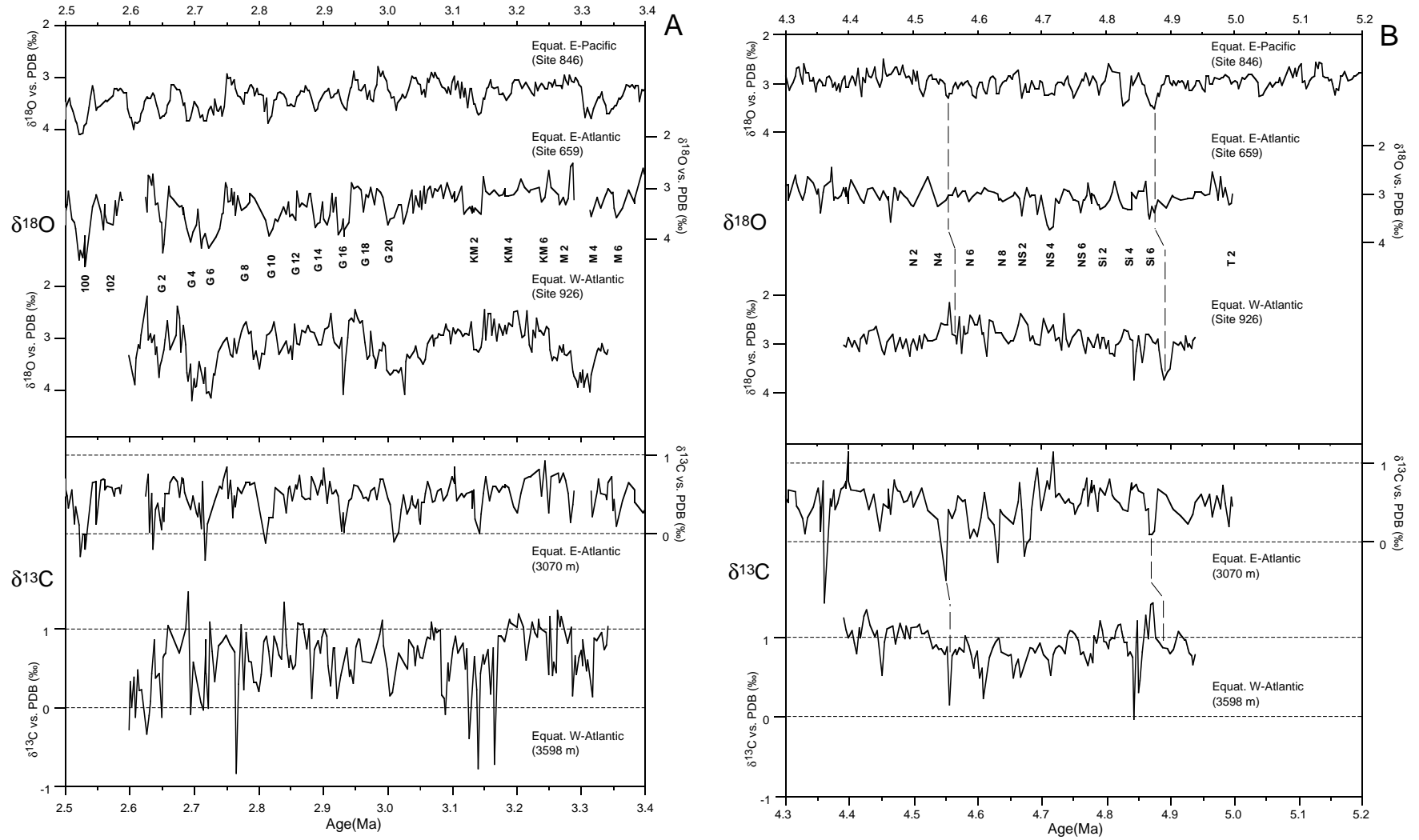


Figure 8. Comparison of Pliocene benthic  $\delta^{18}\text{O}$  and  $\delta^{13}\text{C}$  records from Sites 926, 846 (Shackleton et al., 1995) and 659 (Tiedemann et al., 1994). **A.** 2.5–3.4 Ma. **B.** 4.3–5.2 Ma. Isotope stages are numbered for orientation. Capital letters in front of the isotope stage numbers identify the magnetic polarity interval (G = Gauss, KM = Kaena–Mammoth, M = Mammoth, N = Nunivak, NS = Nunivak–Sidufjall, Si = Sidufjall).

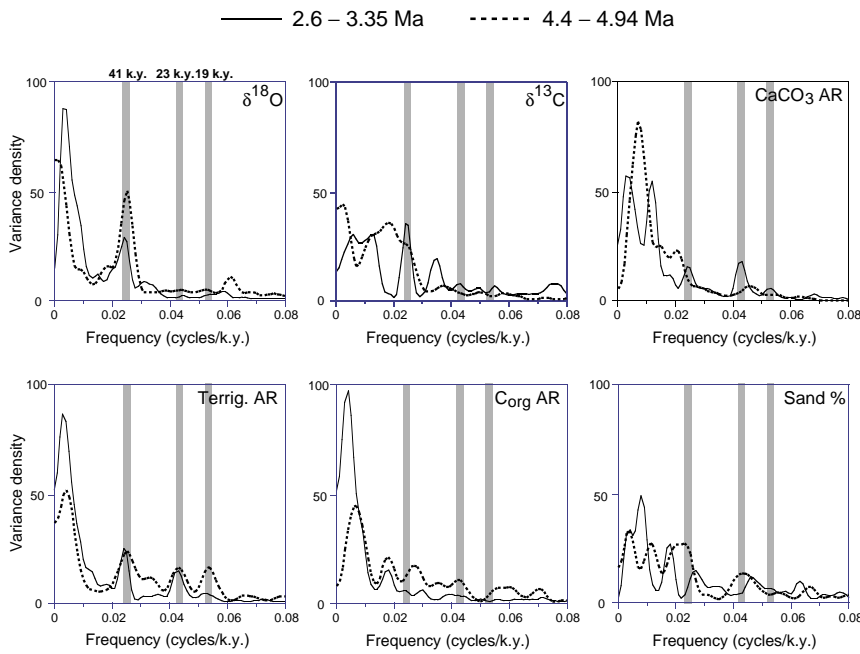


Figure 9. Site 926 frequency spectra of various climate proxy records for middle and early Pliocene time intervals:  $\delta^{18}\text{O}$ ,  $\delta^{13}\text{C}$ , accumulation rates (AR) of  $\text{CaCO}_3$ , siliciclastics (terrigenous), organic carbon ( $\text{C}_{\text{org}}$ ), and sand percentages (as percent of total  $\text{CaCO}_3$ ).

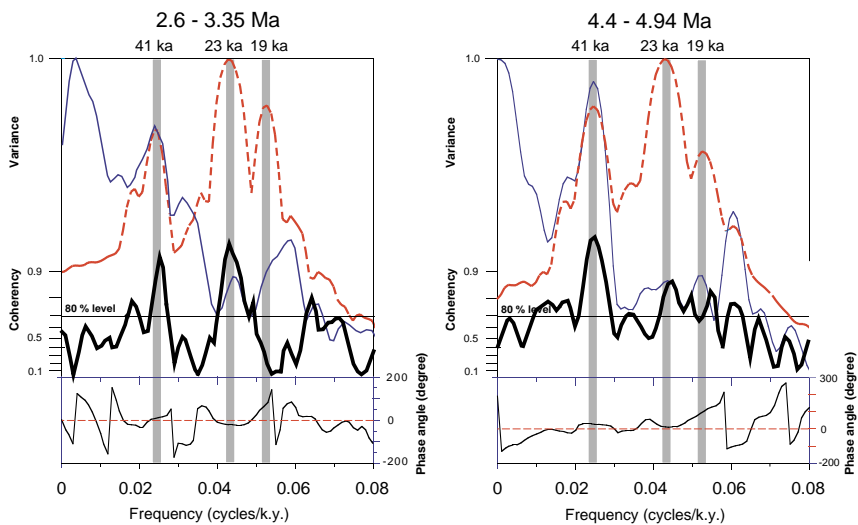


Figure 10. Top: Spectral density and cross-coherency between northern hemisphere summer insolation and the benthic  $\delta^{18}\text{O}$  record from Site 926 over the time intervals 2.6–3.35 Ma and 4.4–4.94 Ma. Bottom: Phase angle vs. frequency plot. Insolation maxima are directly compared with ice volume minima (the sign of  $\delta^{18}\text{O}$  is reversed to indicate minimum ice volume). Positive phase angles indicate that ice volume lag insolation maxima. Obliquity and precessional frequency bands are shaded.

which are also prominent in the sand content record from Site 926. This may indicate a coupling between remineralization and carbonate dissolution, because the decay of organic matter will reduce the carbonate ion concentration in the pore water and, hence, the carbonate preservation (Archer and Maier-Reimer, 1994). The early Pliocene is marked by extremely low organic carbon accumulation rates of  $<0.05 \text{ g/m}^2/\text{yr}$ . During the middle Pliocene, the accumulation rates and amplitude variations are twice as high. The organic carbon records indicate a slight increase from 3.25 to 2.6 Ma. Larger differences in absolute organic carbon contents and accumulation rates between both sites occur only during the middle Pliocene, with higher values at the shallower Site 927. This coincides with higher terrigenous accumulation rates at Site 927 and lower terrigenous accumulation rates at Site 926. Maxima in organic carbon percentages and accumulation rates correspond to maxima in terrigenous sediment input. From this, we cannot exclude that the major proportion of the organic carbon arrived by terrigenous sediment supply at Ceara Rise and probably consists mainly of terrigenous organic carbon, rather than indicating fluctuations in paleoproductivity.

### Siliciclastic Accumulation Rates

During the middle Pliocene, the supply of terrigenous sediments from the Amazon drainage basin is, on average, increased by a factor of two compared to the early Pliocene time interval (Fig. 14). Furthermore, it is recognized that, during both time intervals, the more northerly Sites 927–929, because of their proximity to the Amazon River outflow, have slightly higher siliciclastic accumulation rates than the southerly Sites 925 and 926.

The amplitude fluctuations of the siliciclastic accumulation rates are also different in both time intervals. From 3.3 to 2.6 Ma, the rates fluctuated from 6 to  $29 \text{ g/m}^2/\text{yr}$  and have high amplitudes. In contrast, the rates of the warmer time interval from 5.1 to 4.4 Ma have lower amplitudes and the rates fluctuated from 3 to  $21 \text{ g/m}^2/\text{yr}$ . The higher amplitudes in the middle Pliocene are paralleled by higher amplitudes in the magnetic susceptibility records (Fig. 4), which are also a good proxy for terrigenous sediment supply. During the middle Pliocene, cyclic fluctuations of the siliciclastic accumulation rates respond with nearly equal concentration of variance to the precession

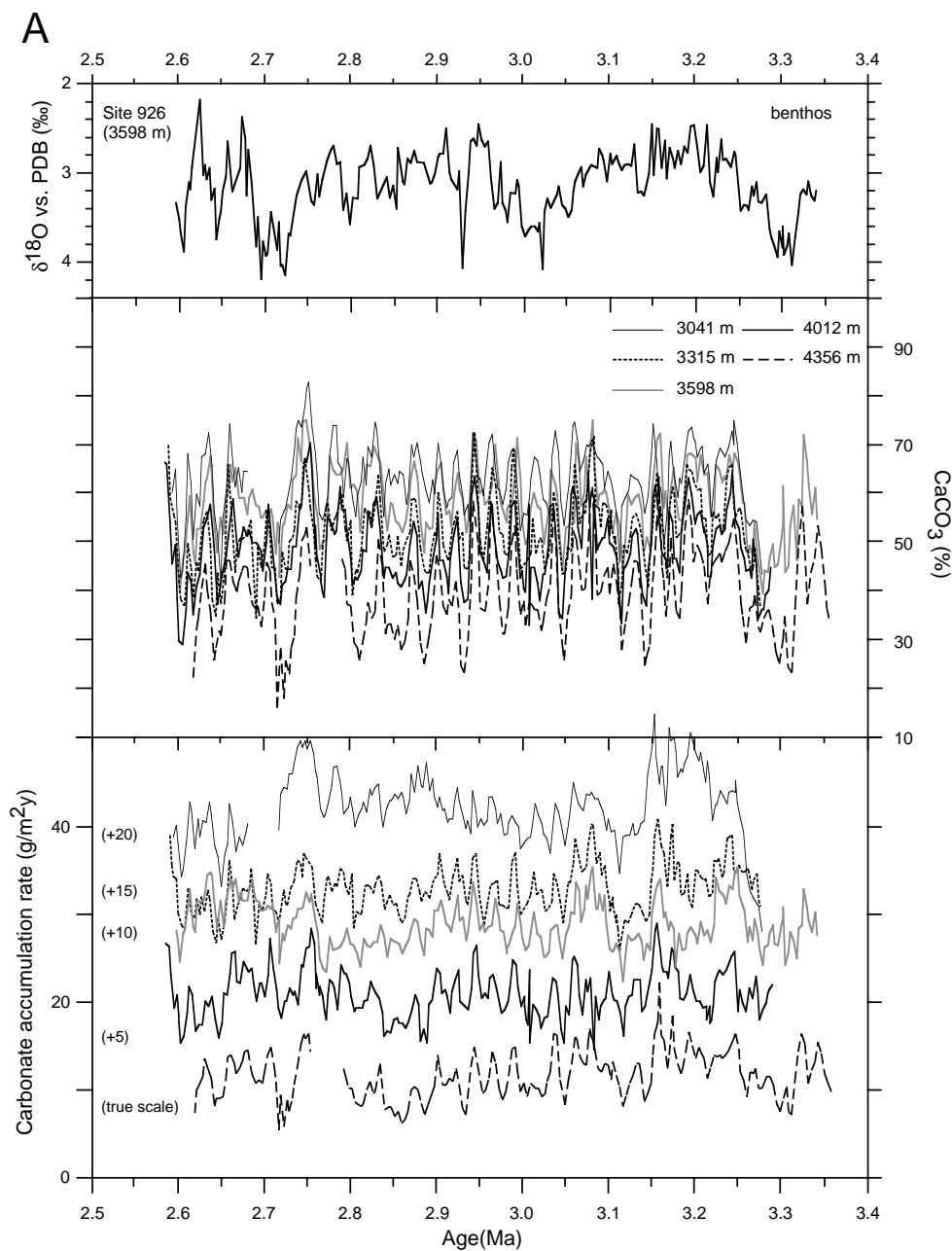


Figure 11. Variations of Pliocene carbonate contents and accumulation rates at Sites 925–929 (3041–4356 m water depth). **A.** 2.6–3.3 Ma. **B.** 4.4–5.1 Ma. The benthic  $\delta^{18}\text{O}$  record from Site 926 is plotted on top for comparison. Carbonate accumulation rates were shifted as indicated to facilitate graphical presentation.

and obliquity periods of orbital forcing. In contrast, the cyclic fluctuations in the early Pliocene are dominated by the precession. Cross-spectral analyses between the siliciclastic accumulation rates and the  $\delta^{18}\text{O}$  record indicate that for both time intervals the supply of terrigenous material parallels ice volume.

## DISCUSSION

### Pliocene Carbonate Preservation Patterns in the Western Equatorial Atlantic

The Pliocene proxy records of deep-water chemistry document that deep-water carbonate dissolution in the equatorial West Atlantic was stronger during the early Pliocene (5–4.5 Ma) than during the

middle Pliocene (3.3–2.6 Ma). This is indicated by (1) lower carbonate accumulation rates at the deeper Sites 928–929, (2) a greater loss of carbonate between 3000 and 4300 m (on average  $18 \text{ g/m}^2/\text{yr}$  vs.  $10 \text{ g/m}^2/\text{yr}$ ), and (3) lower sand contents between 3600 and 4300 m. The bathymetric differences in the sand contents suggest that the lysocline was on average about 200 m shallower during the early Pliocene. Several factors may be responsible for these differences in carbonate preservation including climatic driven changes in deep-water circulation, changes in sea level, variations in productivity, and the closure of the Panama Isthmus. Changes in carbonate productivity as a major cause for the difference in carbonate dissolution between early and middle Pliocene are regarded as minor, because the lower Sites 925–927, well above the lysocline, indicate on average no difference in carbonate accumulation rates.

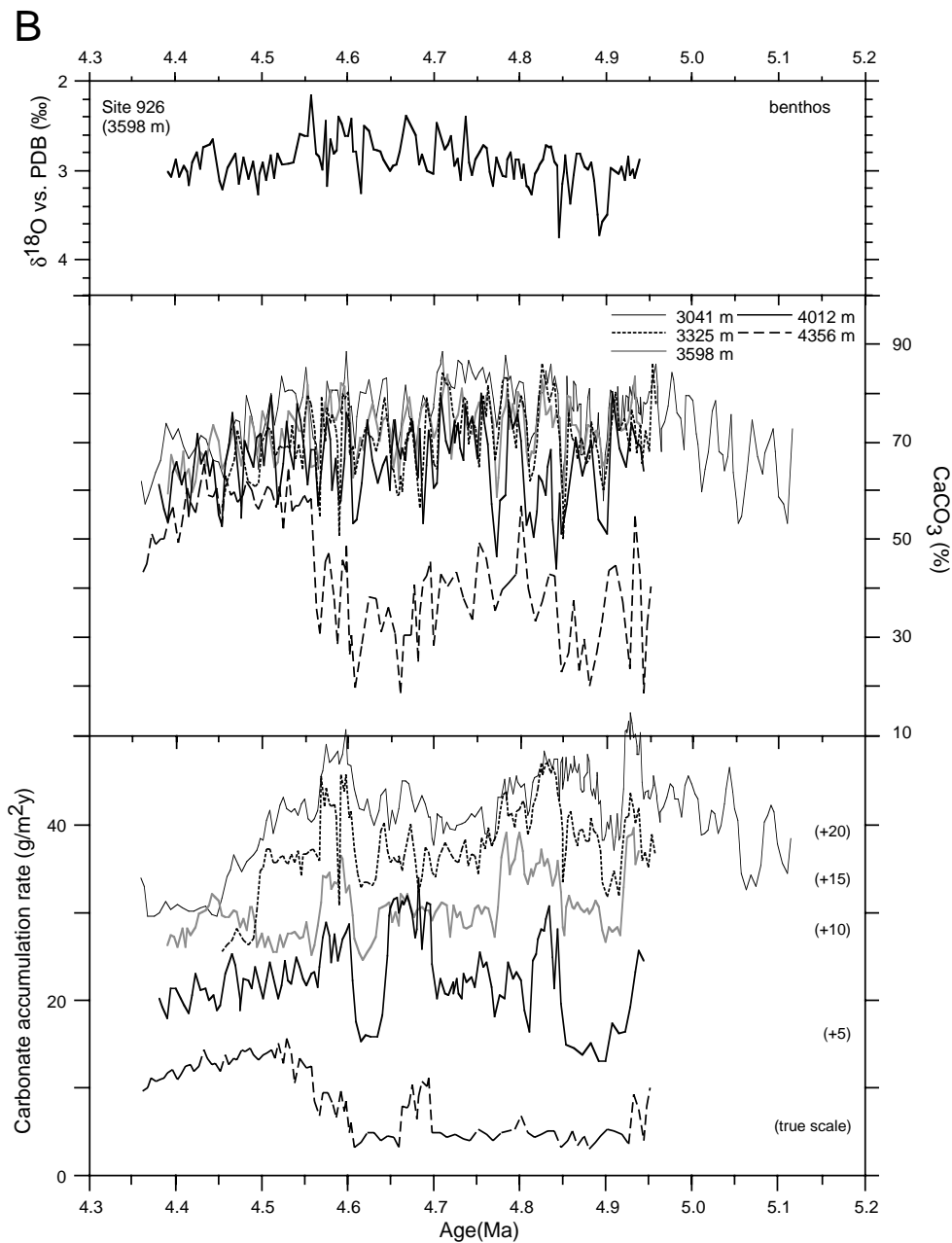


Figure 11 (continued).

Several studies have demonstrated that Pleistocene fluctuations in Atlantic carbonate preservation were linked to the rate of NADW formation, whereas glacial suppressions caused higher carbonate dissolution in the deep Atlantic in response to a greater proportion of carbonate aggressive AABW in the Atlantic. A Pliocene–Pleistocene global comparison of benthic  $\delta^{13}\text{C}$  records (Raymo et al., 1990b, 1992) suggested that the middle Pliocene global cooling led to gradually stronger suppression of NADW production and that the North Atlantic prior to the major northern hemisphere glaciation, was probably characterized by vigorous thermohaline circulation. At Ceara Rise, the long-term decrease in glacial sand contents below 4000 m water depth and the gradual shoaling of the lysocline from 3.3 to 2.6 Ma coincides with decreasing carbonate contents in the North Atlantic (Raymo et al., 1989) and with progressively greater ice volume, lower sea level, cooler climate, and with an increasing influence of

southern source deep-water in the Atlantic. During the middle Pliocene interglacials, no evidence for increased carbonate dissolution occurred in the equatorial West Atlantic.

General circulation model experiments that examined the warmer Pliocene climate prior to the intensification of northern hemisphere glaciation suggested a strengthening of the thermohaline circulation as a result of a salinity increase in the source area of NADW production (Raymo et al., 1990a; Chandler et al., 1994). The prediction of enhanced thermohaline circulation in the North Atlantic during the warmer period of the Pliocene is not reflected by our results. If changes in deep-water circulation have controlled the preservation/dissolution pattern at Ceara Rise, the long-term maximum of enhanced carbonate dissolution during the warm early Pliocene (5–4.5 Ma) would suggest the opposite, a suppression in NADW production and a stronger influence of southern source deep-waters.

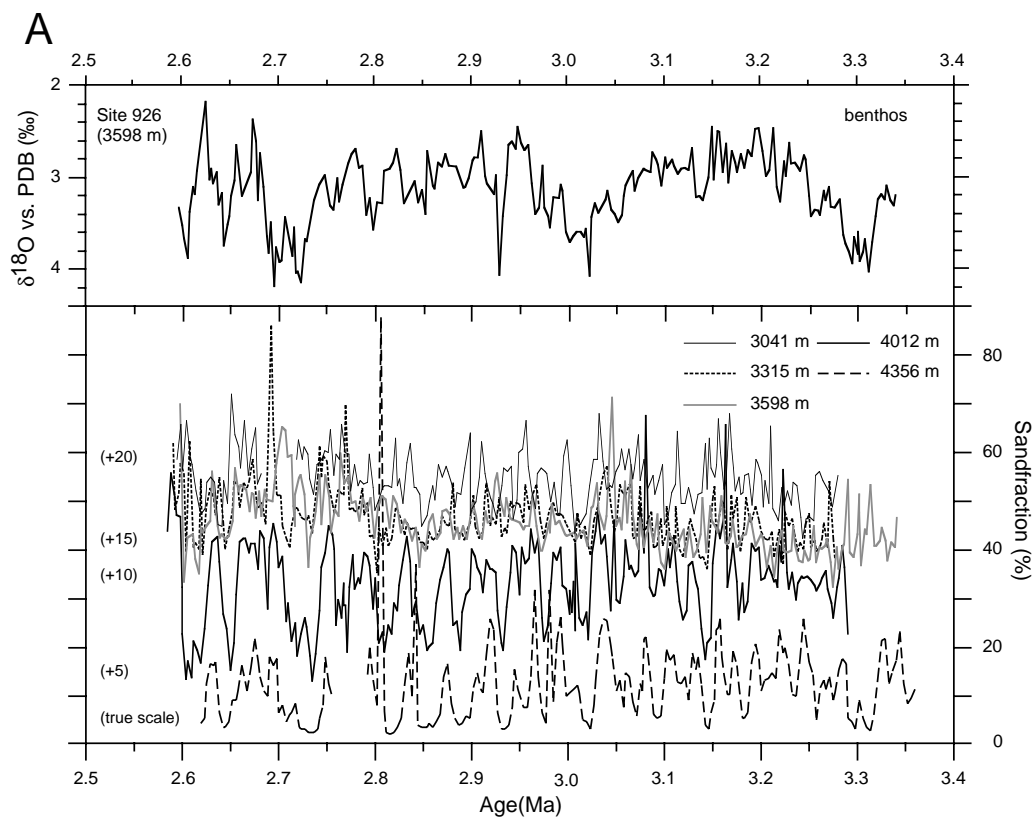


Figure 12. Variations of Pliocene sand contents at Sites 925–929 (3041–4356 m water depth). **A.** 2.6–3.3 Ma. **B.** 4.4–5.1 Ma. The content of the sand fraction  $>63 \mu\text{m}$  is given as percent of total  $\text{CaCO}_3$  and indicative of changes in carbonate dissolution. The benthic  $\delta^{18}\text{O}$  record from Site 926 is plotted on top for comparison. Sand contents were shifted as indicated to facilitate graphical presentation.

The key to understanding is possibly an additional mechanism that prevented an increase in surface salinities in the Norwegian-Greenland and Labrador Seas during the early Pliocene and, thus, lowered the formation of NADW. Strong evidence exists for an open Panama Isthmus during the early Pliocene. A comparison between planktonic  $\delta^{18}\text{O}$  records from the eastern equatorial Pacific and the Caribbean (Keigwin, 1982) indicate that, prior to about 4.2 Ma, the isotope values were the same at both sites (to adjust for the astronomically tuned time scale, the conventional age of 4.2 Ma should be older by about 0.4 Ma; Hilgen, 1991). After 4.2 Ma, the Caribbean  $\delta^{18}\text{O}$  value became significantly heavier than in the eastern Pacific, which was interpreted to reflect an increase in Caribbean surface salinity due to a restricted surface-water communication through the Panama Isthmus. An increasing abundance of high-salinity-tolerant planktonic species in the Caribbean since 4.2 Ma has been reported by Keller et al. (1989). As a result, the Gulf Stream and the thermohaline circulation strengthened in response to a gradual emergence of the isthmus. This scenario is corroborated by the results from an ocean general circulation model that examined changes in ocean circulation patterns with an opened/closed Central American isthmus (Maier-Reimer et al., 1990). With an open isthmus during the early Pliocene, lower salinity waters from the Pacific diluted North Atlantic surface waters and caused a significant reduction in NADW formation. The model results also predicted a higher dissolution of Atlantic carbonate and a better preservation of Pacific carbonate as long as the isthmus was open. High carbonate accumulation rates are known from the equatorial Pacific (Berger et al., 1993; Hagelberg et al., 1995), which decreased from the middle Miocene towards the Pliocene. An open Central American isthmus may explain the persistently strong carbonate dissolution at Ceara Rise since the late Miocene (Curry,

Shackleton, Richter, et al., 1995) and the following increase in carbonate preservation at about 4.6 Ma (Figs. 11B, 12B), when the exchange of surface water started to decrease significantly.

We attribute the short-term fluctuations in carbonate preservation to high latitude, climatically induced changes in deep-water circulation that led to a cyclic shoaling and deepening of the lysocline at a 41-k.y.-rhythm in response to vertical movements of the mixing zone between NADW and AABW. This is suggested by the spectral and cross-spectral results between the sand records, as a sensitive indicator of carbonate dissolution, and the benthic  $\delta^{18}\text{O}$  record, indicative of changes in ice volume. The bathymetric comparison of sand frequency spectra between 3000 and 4300 m water depth indicate for the middle Pliocene dominant precession cycles at shallower depth and a strong overprint of the 41-k.y.-cycle with increasing water depth, and which dominates below 4000 m (Fig. 13). The strongest overprint occurs at Site 928 (4012 m water depth), which was mostly affected by fluctuations in the lysocline depth. The dominance of the precession cycles that occur in the spectra of the sand content records (Fig. 13) and in the carbonate accumulation rate record (Fig. 9) for water masses well above the lysocline may be indicative of Pliocene changes in carbonate production and carbonate flux.

Results from cross-spectral analyses (Table 1) clearly indicate that the mixing between southern and northern source ocean water controlled the temporal dissolution pattern in the equatorial West Atlantic during the middle Pliocene. At the shallowest Site 925, middle Pliocene maxima in carbonate preservation (sand content maxima) were in phase with ice volume minima at the obliquity frequency band (Fig. 15, Table 1), which reflects the “Atlantic-type” interglacial spikes of carbonate preservation (Olausson, 1965; Ruddiman et al., 1988). Below 4000 m water depth, however, which is close to the

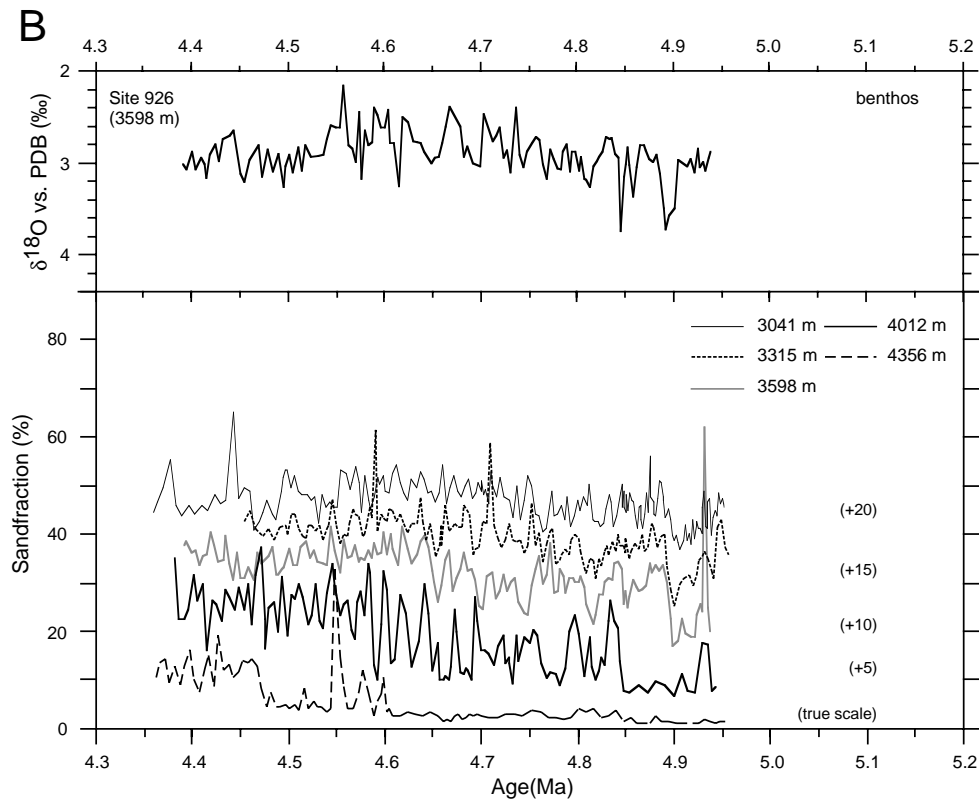


Figure 12 (continued).

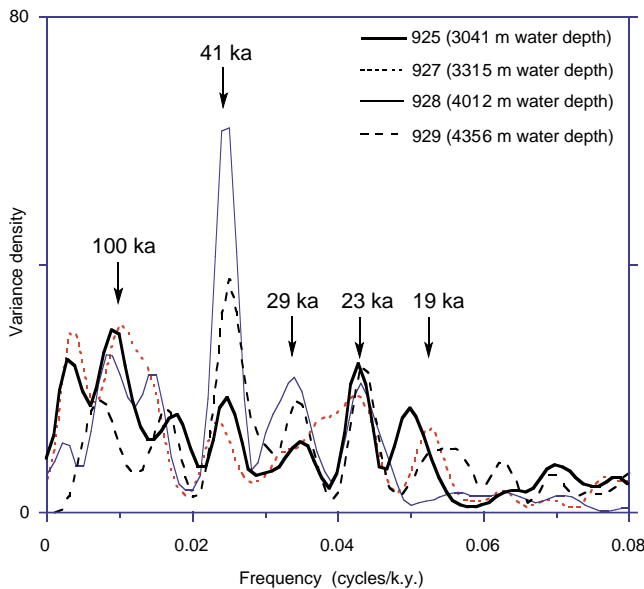


Figure 13. Frequency spectra of sand contents with increasing water depth from 3041 to 4356 m, Sites 925–929. Dominant periods of precession (19 and 23 ka), obliquity (41 ka), and eccentricity (100 ka) are indicated.

modern mixing zone between NADW and AABW, preservation maxima started to lead ice volume minima by  $-38^\circ$  at 4012 m water depth, and by  $-73^\circ$  at 4356 m water depth. This phasing clearly indicates a mixing zone between southern and northern source deep-water, whereas maximum dissolution in the southern source deep-water occurred during ice growth about 8 k.y. earlier than in the intermedi-

ate water (Fig. 15). We attribute the observed phase difference to the chemical asymmetry (out-of-phase relationship) between Atlantic and Pacific, whereas the AABW transferred the early dissolution signal of the Southern Ocean into the equatorial Atlantic. The Pliocene phasing of southern source ocean deep-water to changes in ice volume has been examined by Hagelberg et al. (1995). They used GRAPE density records from the equatorial East Pacific to calculate carbonate percentages and tried to separate the dissolution signal through the use of empirical orthogonal function (EOF) analyses. They found two modes, the second one possibly indicative of carbonate dissolution. Significant coherence with ice volume occurred for the time interval 4–3 Ma, where dissolution maxima lag ice volume minima by about 17 k.y. Additional results, that are based on more reliable indicators of dissolution than carbonate percentages, such as coarse fraction percentages, fragment ratios from coarse fractions or differences in planktonic species compositions according to their resistance to dissolution (Berger, 1970) only exist for Pleistocene records (0–0.8 Ma). Le and Shackleton (1992) reported for the deep equatorial West Pacific that dissolution maxima lag ice volume minima by 9.5–15 k.y. at orbital obliquity, whereas Peterson and Prell (1985) found a lag of about 12 k.y. for the eastern equatorial Indian Ocean. Harris et al. (this volume) used reflectance and magnetic susceptibility records from Ceara Rise to estimate carbonate percentages. They used the ratio of carbonate accumulation rates Site 929/926 as a dissolution index and found that dissolution maxima lag ice volume minima by about 13 k.y. during the last 1 Ma. If we interpret our results in terms of dissolution ( $-73^\circ + 180^\circ$ ), then dissolution maxima at the deepest site of the Ceara Rise transect lag ice volume minima by about 12 k.y. Although this would be consistent with the results cited above and could explain the observed phasing differences in the deep equatorial West Atlantic, it is questionable if the early dissolution events occurred in phase with changes in Atlantic deep water circulation. This would suggest an early shoaling of the upper surface

**Table 1. Results of cross-spectral analyses between various Leg 154 proxies at the main orbital frequencies.**

X-variable	vs.	Y-variable	2.6–3.3 Ma		4.4–5 Ma	
			Obliquity coherency phase	Precession coherency phase	Obliquity coherency phase	Precession coherency phase
Insolation		– $\delta^{18}\text{O}$ (Site 926)	0.94 +10 $\pm$ 10	0.96 (–22 $\pm$ 8)*	0.96 +22 $\pm$ 8	
– $\delta^{18}\text{O}$ (Site 926)		$\delta^{13}\text{C}$ (Site 926)	0.83 +38 $\pm$ 18	0.83 (+35 $\pm$ 18)*		0.87 (+5 $\pm$ 15)*
Insolation		Sand (Site 925)	0.75 +9 $\pm$ 24	0.71 +148 $\pm$ 26		
Insolation		Sand (Site 927)	( 0.57 ) <sup>#</sup> +39 $\pm$ 37	0.73 +38 $\pm$ 28		
Insolation		Sand (Site 928)	0.97 –22 $\pm$ 7	0.96 +25 $\pm$ 7		
Insolation		Sand (Site 929)	0.90 –66 $\pm$ 14	0.88 +9 $\pm$ 15		
– $\delta^{18}\text{O}$ (Site 926)		Sand (Site 925)	0.71 +4 $\pm$ 26	0.60 –		
– $\delta^{18}\text{O}$ (Site 926)		Sand (Site 927)	( 0.68 ) <sup>#</sup> +12 $\pm$ 27	0.56 –		
– $\delta^{18}\text{O}$ (Site 926)		Sand (Site 928)	0.95 –38 $\pm$ 10	0.84 (+45 $\pm$ 18)*		
– $\delta^{18}\text{O}$ (Site 926)		Sand (Site 929)	0.75 –73 $\pm$ 24	0.83 (+15 $\pm$ 19)*		
CaCO <sub>3</sub> AR (Site 925)		Sand (Site 925)	– –	0.87 +167 $\pm$ 15		
CaCO <sub>3</sub> AR (Site 927)		Sand (Site 927)	0.73 +56 $\pm$ 25	( 0.64 ) <sup>#</sup> +54 $\pm$ 30		
CaCO <sub>3</sub> AR (Site 928)		Sand (Site 928)	0.92 –32 $\pm$ 12	0.97 +24 $\pm$ 6		
CaCO <sub>3</sub> AR (Site 929)		Sand (Site 929)	0.87 –51 $\pm$ 16	0.93 +25 $\pm$ 11		
Insolation		Silicicl. AR (Site 926)	0.96 –174 $\pm$ 8	0.97 +171 $\pm$ 7	0.86 –141 $\pm$ 16	0.98 –166 $\pm$ 6
– $\delta^{18}\text{O}$ (Site 926)		Silicicl. AR (Site 926)	0.96 +171 $\pm$ 8	0.92 (–167 $\pm$ 12)*	0.83 –162 $\pm$ 18	0.88 (–178 $\pm$ 14)*

Notes: The sign of  $\delta^{18}\text{O}$  is reversed to indicate minimum ice volume. Positive (negative) phase angles implies that Y lags (leads) X. For example, sand content maxima at Site 929 lead ice volume minima ( $\delta^{18}\text{O}$  Site 926) or insolation maxima by  $-73^\circ$  or  $-66^\circ$ , respectively, at the obliquity frequency band. \* = these phase estimates should be considered with great caution, because the variance for  $\delta^{18}\text{O}$  fluctuations at the precessional bands is less than 5%. # = coherency and phase estimates are just below the 80% confidence levels. Silicicl. AR = siliciclastic accumulation rate.

of AABW in the equatorial Atlantic in response to a decreased export of NADW, that occurred several thousand years before the ice volume maximum.

The phase relationships for the precession band indicate no water depth relationship between 3300 m and 4350 m (considering the error limits), and sand maxima slightly lag insolation maxima by about 1.5 k.y. (Table 1). This suggests that changes in deep-water circulation and/or the redistribution of carbonate ions in the equatorial West Atlantic mainly operated at obliquity cycles during the middle Pliocene.

### Pliocene Changes in the Supply of Amazon Siliciclastics

The late Neogene evolution of Amazon sediment discharge to Ceara Rise is marked by a long-term increase since the late Miocene (Curry, Shackleton, Richter, et al., 1995). This increase is also reflected in the Pliocene time intervals with lower siliciclastic accumulation rates in the early Pliocene and higher rates during the middle Pliocene (Fig. 14). The Pliocene increase of the siliciclastic accumulation rates may result from enhanced erosion of the Andes caused by accelerated uplift (Benjamin et al., 1987) and/or global cooling. However, we cannot ascertain a long-term connection between the middle Pliocene intensification of northern hemisphere glaciation and the terrigenous sediment supply to the Ceara Rise (Fig. 14A). In addition, results from general circulation models provide no evidence that Pliocene changes in Arctic ice cover were responsible for significant changes in tropical precipitation that would effect the extension

of tropical rain forests and the fluvial runoff (Crowley et al., 1994; Chandler et al., 1994).

During both intervals, cyclic fluctuations of the siliciclastic accumulation rates respond with nearly equal concentration of variance to the precession and obliquity periods of orbital forcing, whereas cyclic changes in the benthic oxygen isotope record are dominated by the obliquity cycle (Fig. 9). Cross-spectral analyses between the siliciclastic accumulation rates and the  $\delta^{18}\text{O}$  record indicate an in-phase relationship at orbital obliquity with maxima in the supply of terrigenous material at ice volume maxima (Table 1). Hence, the 41-k.y.-fluctuations in the supply of Amazon siliciclastics may result from sea-level changes as suggested by Flood, Piper, Klaus, et al. (1995). However, benthic oxygen isotopes, as an indicator for change in ice volume, show no significant response to orbital precession (Fig. 9). This suggests that climatological changes in South America and/or changes in the intensity of the North Brazilian Coastal Current are strong candidates in the control of the precessional flux of terrigenous material to Ceara Rise.

## CONCLUSIONS

1. At Sites 925–928, an orbitally tuned time scale was generated for the Pliocene from 5 to 2.5 Ma by correlating precessional magnetic susceptibility cycles to the  $65^\circ\text{N}$  summer insolation record that was based on the astronomical solution of Laskar

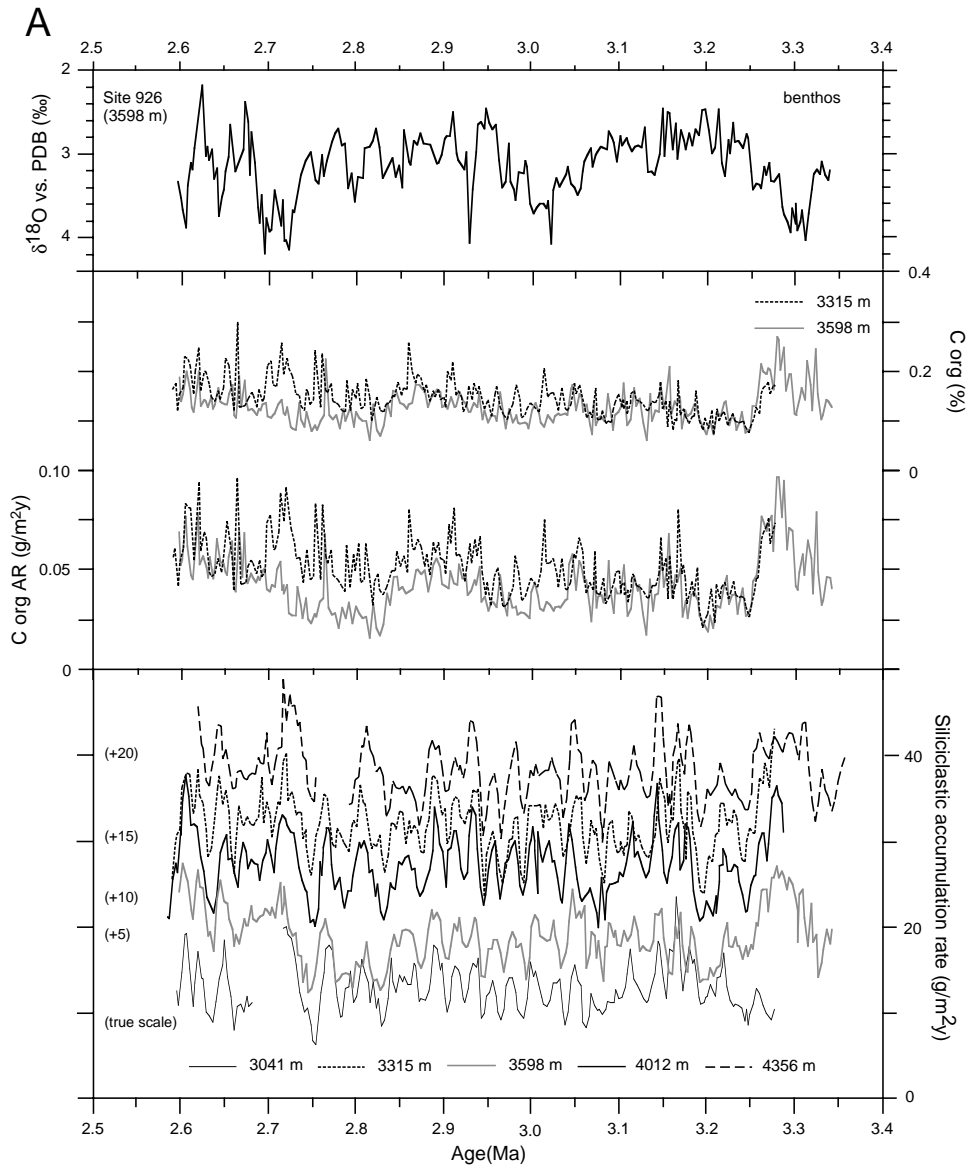


Figure 14. Variations of organic carbon contents and accumulation rates, and siliciclastic accumulation rates at Sites 925–929 (3041–4356 m water depth). **A.** 2.6–3.3 Ma. **B.** 4.4–5.1 Ma. The benthic  $\delta^{18}\text{O}$  record from Site 926 is plotted on top for comparison. Siliciclastic accumulation rates were shifted as indicated to facilitate graphical presentation (continued next page).

et al. (1993). The tuning enabled a high resolution comparison between various proxy records that monitor the different aspects of the Pliocene carbonate production-preservation-dissolution system at Ceara Rise, as well as changes in the supply of Amazon sediments.

2. The intensification of northern hemisphere glaciation from 3.3 to 2.6 Ma was paralleled by a gradual decrease in glacial sand contents below 4000 m water depth and the gradual shoaling of the lysocline. This coincides with progressively greater ice volume, lower sea level, cooler climate, and with an increasing influence of southern-source deep-water in the Atlantic. During the middle Pliocene interglacials, no evidence for increased carbonate dissolution occurred in the equatorial West Atlantic.
3. In the equatorial West Atlantic, middle Pliocene fluctuations in carbonate preservation were linked to high-latitude, climatically induced, changes in deep-water circulation that led to a cyclic shoaling and deepening of the lysocline at a 41-k.y.-rhythm in response to vertical movements of the mixing zone

between NADW and AABW. Maxima in carbonate dissolution at 4356 m water depth lead maxima ice volume by 8 k.y. at the obliquity band and suggest an early response to climate change in the Southern Ocean. This phasing decreased towards shallower water depths returning to the “Atlantic type” of carbonate preservation (in-phase with changes in global ice volume). The dissolution fluctuations are consistent with Boyle’s nutrient rearrangement model (Boyle, 1992).

4. In contrast to the deeper sediment records, fluctuations in carbonate accumulation rates and sand contents in less undersaturated water masses well above the lysocline are dominated by 23-k.y.- and 19-k.y.-cyclicities, indicating that carbonate productivity and flux were mainly controlled by precessional climate forcing during the middle Pliocene.
5. The early warm Pliocene, from 5 to 4.6 Ma, was marked by a greater loss of carbonate between 3000 and 4300 m water depth and a lysocline depth of about 200 m shallower than during the middle Pliocene. This time interval of stronger carbonate dissolution may result from an open Central American

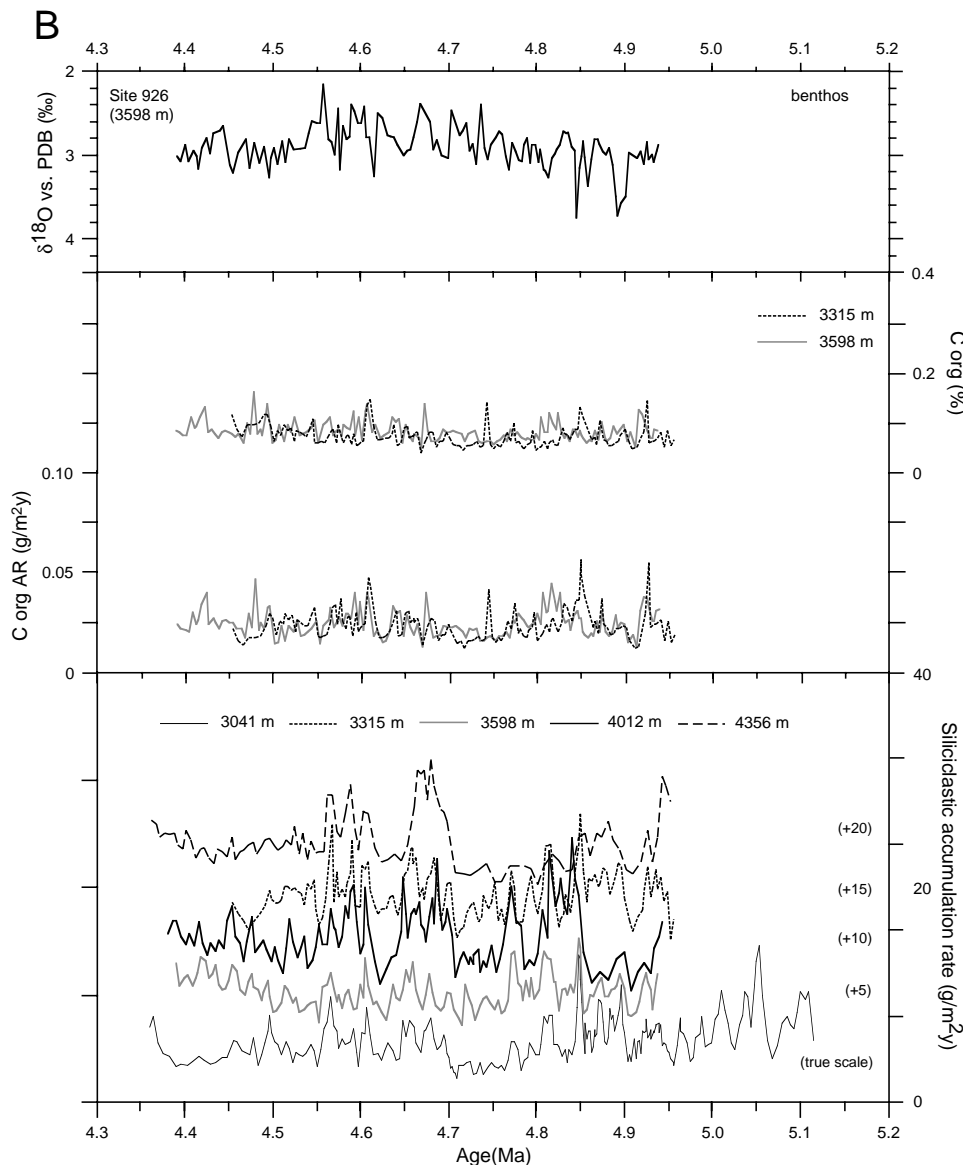


Figure 14 (continued).

isthmus, when NADW production was suppressed. A distinct increase in carbonate preservation occurred at about 4.6 Ma and may reflect a restricted surface-water communication through the Panama Isthmus, as suggested by Keigwin (1982).

6. At Ceara Rise, the fluctuations in the supply of Amazon sediments during the early and middle Pliocene were dominated by precessional and obliquity periods. The 41-k.y.-fluctuations were in phase with benthic  $\delta^{18}\text{O}$  and, hence, may result from sea-level changes. At the precessional band, however, benthic oxygen isotopes showed no response to orbital precession. This suggests that climatological changes in South America and/or changes in the intensity of the North Brazilian Coastal Current were strong candidates in controlling the precessional flux of terrigenous material to Ceara Rise.

#### ACKNOWLEDGMENTS

We thank the Ocean Drilling Program and the shipboard scientists of ODP Leg 154 who made this study possible. We wish to thank W.

Berger, T. Bickert, R. Keir, and R. Zahn for constructive criticisms that helped to improve the manuscript. We gratefully acknowledge the cooperation with M. Segl, who supervised the operation of the automatized Bremen mass spectrometer with special care, and we thank K. Schirmer, A. Sturm, V. Strauß, and J. Meyer. This study was supported by the Deutsche Forschungsgemeinschaft (Ti 240/1-1).

#### REFERENCES

- Archer, D.E., and Maier-Reimer, E., 1994. Effect of deep-sea sedimentary calcite preservation on atmospheric  $\text{CO}_2$  concentration. *Nature*, 367:260–263.
- Benjamin, M., Johnson, N.M., and Naeser, C.W., 1987. Recent rapid uplift in the Bolivian Andes: evidence from fission-track dating. *Geology*, 15:680–683.
- Berger, A., and Loutre, M.F., 1991. Insolation values for the climate of the last 10 million years. *Quat. Sci. Rev.*, 10:297–317.
- Berger, W.H., 1970. Biogenous deep-sea sediments: fractionation by deep-sea circulation. *Geol. Soc. Am. Bull.*, 81:1385–1401.
- Berger, W.H., 1982. Increase of carbon dioxide in the atmosphere during deglaciation: the coral reef hypothesis. *Naturwissenschaften*, 69:87–88.

- Berger, W.H., Burke, S., and Vincent, E., 1987. Glacial-Holocene transition: climate pulsations and sporadic shutdown of NADW production. In Berger, W.H., and Labeysrie, L.D. (Eds.), *Abrupt Climatic Change: Evidence and Implications*: Dordrecht (Reidel), 279–297.
- Berger, W.H., Leckie, R.M., Janecek, T.R., Stax, R., and Takayama, T., 1993. Neogene carbonate sedimentation on Ontong Java Plateau: highlights and open questions. In Berger, W.H., Kroenke, L.W., Mayer, L.A., et al., *Proc. ODP, Sci. Results*, 130: College Station, TX (Ocean Drilling Program), 711–744.
- Beveridge, N.A.S., Elderfield, H., and Shackleton, N.J., 1995. Deep thermohaline circulation in the low latitude Atlantic during the last glacial. *Paleoceanography*, 10:643–660.
- Bickert, T., 1992. Rekonstruktion der spätquartären Bodenwasserzirkulation im östlichen Südatlantik über stabile Isotope benthischer Foraminiferen [Ph.D. dissert.]. Universität Bremen.
- Boyle, E.A., 1988. The role of vertical chemical fractionation in controlling late Quaternary atmospheric carbon dioxide. *J. Geophys. Res.*, 93:15701–15714.
- Boyle, E.A., 1992. Cadmium and  $\delta^{13}\text{C}$  paleochemical ocean distributions during the stage 2 glacial maximum. *Annu. Rev. Earth Planet. Sci.*, 20:245–287.
- Broecker, W.S., 1982. Ocean chemistry during glacial time. *Geochim. Cosmochim. Acta*, 46:1689–1705.
- Broecker, W.S., and Peng, T.-H., 1989. The cause of the glacial to interglacial atmospheric  $\text{CO}_2$  change: a polar alkalinity hypothesis. *Global Biogeochem. Cycles*, 3:215–239.
- Broecker, W.S., and Takahashi, T., 1978. The relationship between lysocline depth and in-situ carbonate ion concentration. *Deep-Sea Res. Part A*, 25:65–95.
- Carlson, T.N., and Prospero, J.M., 1972. The large-scale movement of Saharan Air outbreaks over the northern equatorial Atlantic. *J. Appl. Meteorol.*, 11:283–297.
- Chandler, M., Rind, D., and Thompson, R., 1994. Joint investigations of the middle Pliocene climate II: GISS GCM Northern Hemisphere results. *Global Planet. Change*, 9:197–219.
- Chen, J., Farrell, J.W., Murray, D.W., and Prell, W.L., 1995. Timescale and paleoceanographic implications of a 3.6 m.y. oxygen isotope record from the northeast Indian Ocean (Ocean Drilling Program site 758). *Paleoceanography*, 10:21–47.
- Crowley, T.J., Yip, K.-J. J., and Baum, S.K., 1994. Effect of altered Arctic sea ice and Greenland ice sheet cover on the climate of the GENESIS general circulation model. *Global Planet. Change*, 9:275–288.
- Curry, W.B., and Lohmann, G.P., 1990. Reconstructing past particle fluxes in the tropical Atlantic Ocean. *Paleoceanography*, 5:487–505.
- Curry, W.B., and Miller, K.G., 1989. Oxygen and carbon isotopic variation in Pliocene benthic foraminifers of the equatorial Atlantic. In Ruddiman, W., Sarnthein, M., et al., *Proc. ODP, Sci. Results*, 108: College Station, TX (Ocean Drilling Program), 157–166.
- Curry, W.B., Shackleton, N.J., Richter, C., et al., 1995. *Proc. ODP, Init. Repts.*, 154: College Station, TX (Ocean Drilling Program).
- Dessier, A., and Donguy, J.R., 1994. The sea surface salinity in the tropical Atlantic between  $10^\circ\text{S}$  and  $30^\circ\text{N}$ —seasonal and interannual variations (1977–1989). *Deep-Sea Res.*, 41:81–100.
- Farrell, J.W., III, 1991. Late Neogene palaeoceanography of the central equatorial Pacific: evidence from carbonate preservation and stable isotopes [Ph.D. dissert.]. Brown Univ., Providence, RI.
- Farrell, J.W., and Prell, W.L., 1989. Climatic change and  $\text{CaCO}_3$  preservation: an 800,000 year bathymetric reconstruction from the central equatorial Pacific Ocean. *Paleoceanography*, 4:447–466.
- Farrell, J.W., and Prell, W.L., 1991. Pacific  $\text{CaCO}_3$  preservation and  $\delta^{18}\text{O}$  since 4 Ma: paleoceanic and paleoclimatic implications. *Paleoceanography*, 6:485–498.
- Flood, R.D., Piper, D.J.W., Klaus, A., et al., 1995. *Proc. ODP, Init. Repts.*, 155: College Station, TX (Ocean Drilling Program).
- Hagelberg, T.K., Pisias, N.G., Mayer, L.A., Shackleton, N.J., and Mix, A.C., 1995. Spatial and temporal variability of late Neogene equatorial Pacific carbonate: Leg 138. In Pisias, N.G., Mayer, L.A., Janecek, T.R., Palmer-Julson, A., and van Andel, T.H. (Eds.), *Proc. ODP, Sci. Results*, 138: College Station, TX (Ocean Drilling Program), 321–336.
- Haug, G., 1995. Zur Paläo-Ozeanographie und Sedimentationsgeschichte im Nordwest-Pazifik während der letzten 6 Millionen Jahre (ODP-Site 882) [Ph.D. dissert.]. Universität Kiel.
- Haug, G.H., Maslin, M.A., Sarnthein, M., Stax, R., and Tiedemann, R., 1995. Evolution of northwest Pacific sedimentation patterns since 6 Ma (Site 882). In Rea, D.K., Basov, I.A., Scholl, D.W., and Allan, J.F. (Eds.), *Proc. ODP, Sci. Results*, 145: College Station, TX (Ocean Drilling Program), 293–314.
- Hilgen, F.J., 1991. Extension of the astronomically calibrated (polarity) time scale to the Miocene/Pliocene boundary. *Earth Planet. Sci. Lett.*, 107:349–368.
- Imbrie, J., Hays, J.D., Martinson, D.G., McIntyre, A., Mix, A.C., Morley, J.J., Pisias, N.G., Prell, W.L., and Shackleton, N.J., 1984. The orbital theory of Pleistocene climate: support from a revised chronology of the marine  $\delta^{18}\text{O}$  record. In Berger, A., Imbrie, J., Hays, J., Kukla, G., and Saltzman, B. (Eds.), *Milankovitch and Climate* (Pt. 1), NATO ASI Ser. C, Math Phys. Sci., 126: Dordrecht (D. Reidel), 269–305.
- Imbrie, J., and Imbrie, J.Z., 1980. Modeling the climatic response to orbital variations. *Science*, 207:943–953.
- Jones, G.A., and Ruddiman, W.F., 1982. Assessing the global meltwater spike. *Quat. Res.*, 17:148–172.
- Keigwin, L., 1982. Isotopic paleoceanography of the Caribbean and East Pacific: role of Panama Uplift in late Neogene time. *Science*, 217:350–353.
- Keller, G., Zenker, C.E., and Stone, S.M., 1989. Late Neogene history of the Pacific-Caribbean gateway. *J. South Am. Earth Sci.*, 2:73–108.
- Laskar, J., 1990. The chaotic motion of the solar system: a numerical estimate of the size of the chaotic zones. *Icarus*, 88:266–291.
- Laskar, J., Joutel, F. and Boudin, F., 1993. Orbital, precessional, and insolation quantities for the Earth from -20 Myr to +10 Myr. *Astron. Astrophys.*, 270:522–533.
- Le, J., and Shackleton, N.J., 1992. Carbonate dissolution fluctuations in the western equatorial Pacific during the late Quaternary. *Paleoceanography*, 7:21–42.
- Lourens, L.J., 1994. Astronomical forcing of Mediterranean climate during the last 5.3 million years [Ph.D. dissert.]. Universiteit Utrecht.
- Lourens, L.J., Hilgen, F.J., Zachariasse, W.J., Van Hoof, A.A.M., Antonarakou, A., and Vergnaud-Grazzini, C., 1996. Evaluation of the Plio-Pleistocene astronomical time scale. *Paleoceanography*, 11:391–413.
- Maier-Reimer, E., Mikolajewicz, U. and Crowley, T., 1990. Ocean general circulation model sensitivity experiment with an open Central American Isthmus. *Paleoceanography*, 5:349–366.
- McCorkle, D.C., and Keigwin, L.D., 1994. Depth profiles of  $\delta^{13}\text{C}$  in bottom water and core-top *C. wuellerstorfi* on the Ontong-Java Plateau and Emperor Seamounts. *Paleoceanography*, 9:197–208.
- Metcalfe, W.G., Heezen, B.C., and Stalcup, M.C., 1964. The sill depth of the Mid Atlantic Ridge in the equatorial region. *Deep-Sea Res.*, 11:1–10.
- Moore, T.C., Jr., Pisias, N.G., and Heath, G.R., 1977. Climatic changes and lags in carbonate preservation, sea surface temperature, and global ice volume. In Anderson, N.R., and Malahoff, A. (Eds.), *The Fate of Fossil Fuel  $\text{CO}_2$  in the Oceans*: New York (Plenum), 145–165.
- Nittrouer, C.A., and DeMaster, D.J., 1986. Sedimentary processes on the Amazon continental shelf: past, present and future research. *Cont. Shelf Res.*, 6:5–30.
- Olausson, E., 1965. Evidence of climatic changes in north Atlantic deep sea cores, with remarks on isotopic paleotemperature analysis. *Progr. Oceanogr.*, 3:221–252.
- Oppo, D., and Fairbanks, R.G., 1987. Variability in the deep and intermediate water circulation of the Atlantic Ocean during the past 25,000 years: Northern Hemisphere modulation of the Southern Ocean. *Earth Planet. Sci. Lett.*, 86:1–15.
- Peterson, L.C., and Prell, W.L., 1985. Carbonate preservation and rates of climatic change: an 800 kyr record from the Indian Ocean. In Sundquist, E.T., and Broecker, W.S. (Eds.), *The Carbon Cycle and Atmospheric  $\text{CO}_2$ : Natural Variations, Archean to Present*. Geophys. Monogr., Am. Geophys. Union, 32:251–270.
- Philander, S.G.H., and Pacanowski, R.C., 1986. A model of seasonal cycle in the tropical Atlantic Ocean. *J. Geophys. Res.*, 91:14192–14206.
- Raymo, M.E., Hodell, D., and Jansen, E., 1992. Response of deep ocean circulation to initiation of Northern Hemisphere glaciation (3–2 Ma). *Paleoceanography*, 7:645–672.
- Raymo, M.E., Rind, D., and Ruddiman, W.F., 1990a. Climatic effects of reduced Arctic sea ice limits in the GISS II general circulation model. *Paleoceanography*, 5:367–382.
- Raymo, M.E., Ruddiman, W.F., Backmann, J., Clement, B.M., and Martinson, D.G., 1989. Late Pliocene variations in Northern Hemisphere ice sheets and North Atlantic deep-water circulation. *Paleoceanography*, 4:413–446.
- Raymo, M.E., Ruddiman, W.F., Shackleton, N.J., and Oppo, D.W., 1990b. Evolution of Atlantic-Pacific  $\delta^{13}\text{C}$  gradients over the last 2.5 m.y. *Earth Planet. Sci. Lett.*, 97:353–368.

Richardson, P.L., and Walsh, D., 1986. Mapping climatological seasonal variations of surface currents in the tropical Atlantic using ship drifts. *J. Geophys. Res.*, 91:10357–10550.

Robinson, S.G., Maslin, M.A., and McCave, I.N., 1995. Magnetic susceptibility variations in late Pleistocene deep-sea sediments of the N.E. Atlantic: implications for ice-rafting and paleocirculation at the last glacial maximum. *Paleoceanography*, 10:221–250.

Ruddiman, W.F., Backman, J., Baldauf, J., Hooper, P., Keigwin, L., Miller, K., Raymo, M., and Thomas, E., 1987. Leg 94 paleoenvironmental synthesis. In Ruddiman, W.F., Kidd, R.B., Thomas, E., et al., *Init. Repts. DSDP*, 94: Washington (U.S. Government Printing Office), 1207–1215.

Ruddiman, W., Sarnthein, M., Baldauf, J., et al., 1988. *Proc. ODP, Init. Repts.*, 108 (Sections 1 and 2): College Station, TX (Ocean Drilling Program).

Sarnthein, M., Winn, K., Jung, S., Duplessy, J.-C., Labeyrie, L., Erlenkeuser, H., and Ganssen, G., 1994. Changes in East Atlantic deep-water circulation over the last 30,000 years: eight time-slice reconstructions. *Paleoceanography*, 9:209–267.

Shackleton, N.J., and Hall, M.A., 1984. Oxygen and carbon isotope stratigraphy of Deep Sea Drilling Project Hole 552A: Plio-Pleistocene glacial history. In Roberts, D.G., Schnitker, D., et al., *Init. Repts. DSDP*, 81: Washington (U.S. Govt. Printing Office), 599–609.

Shackleton, N.J., Hall, M.A., and Pate, D., 1995. Pliocene stable isotope stratigraphy of Site 846. In Pisias, N.G., Mayer, L.A., Janecek, T.R., Palmer-Julson, A., and van Andel, T.H. (Eds.), *Proc. ODP, Sci. Results*, 138: College Station, TX (Ocean Drilling Program), 337–355.

Showers, W.J., and Bevis, M., 1988. Amazon Cone isotopic stratigraphy: evidence for the source of the tropical meltwater spike. *Palaeogeogr., Palaeoclimatol., Palaeoecol.*, 64:189–199.

Tiedemann, R., 1991. Acht Millionen Jahre Klimageschichte von Nordwest Afrika und Palaeozeanographie des Angrenzenden Atlantiks: Hochaufosende Zeitreihen von ODP Sites 658–661 [Ph.D. thesis]. *Geol.-Palaeont. Inst., Univ. Kiel*, Ber. 46.

Tiedemann, R., Sarnthein, M., and Shackleton, N.J., 1994. Astronomic timescale for the Pliocene Atlantic  $\delta^{18}\text{O}$  and dust flux records of Ocean Drilling Program Site 659. *Paleoceanography*, 9:619–638.

Turnau, R., and Ledbetter, M.T., 1989. Deep circulation changes in the South Atlantic Ocean: response to initiation of Northern Hemisphere glaciation. *Paleoceanography*, 4:565–583.

Van der Hammen, T., and Absy, M.L., 1994. Amazonia during the last glacial. *Palaeogeogr., Palaeoclimatol., Palaeoecol.*, 109:247–261.

Yasuda, M., Berger, W.H., Wu, G., Burke, S., and Schmidt, H., 1993. Foraminifer preservation record for the last million years: Site 805, Ontong Java Plateau. In Berger, W.H., Kroenke, L.W., Mayer, L.A., et al., *Proc. ODP, Sci. Results*, 130: College Station, TX (Ocean Drilling Program), 491–508.

Date of initial receipt: 11 December 1005

Date of acceptance: 22 August 1996

Ms 154SR-120

Figure 15. Comparison of phase relationships between ice volume and carbonate dissolution proxies for the equatorial west Atlantic and Indo-Pacific in the 41-k.y. frequency band. The phase wheel for the Ceara Rise region (left) indicates that maxima in sand concentration, indicative of carbonate preservation, lead ice volume minima with increasing water depth (about 8 k.y. at 4356 m) during the middle Pliocene. On the other hand, maximum dissolution lags ice volume minimum by 12 k.y. (4356 m). This phase lag is equal to the average lag observed for the equatorial West Pacific (Le and Shackleton, 1992) and Indian Ocean (Peterson and Prell, 1985).

